Assessment of vegetation dynamics in the glacier fore-fields ofthe Swiss Alps based on 30 years of Landsat data

ESS 511 Master's Thesis

Author
Sebastian Röthlin
13-755-285

Supervised by
Dr. Frank Paul
Dr. Rogier De Jong

Faculty representative
Prof. Dr. Andreas Vieli

29.06.2019
Department of Geography, University of Zurich

Abstract

Glacier fore-fields are the dynamic systems that follow glacier retreat. Within this dynamic, the development of a vegetation cover is tied to multiple aspects of the glacier fore-field. Primary vegetation starts to build up soil which is required for further stages of the vegetation succession. Topography and geology affect the availability of light, water and substrate for vegetation to grow on while in turn the plants affect morphological processes by stabilising the ground. Furthermore, vegetation cover changes the spectral properties of the glacier fore-field. This allows observing vegetation development with remote sensing. With a time series of more than 30 years, optical data from the Landsat satellite missions can be used to assess vegetation dynamics in large spatial scales. On the basis of optical data form Landsat 5, 7 and 8, vegetation dynamics have been analysed first in the region of the Morteratsch glacier and in a second step in all the glacier fore-fields of the Swiss Alps. Shapefiles of the outlines of the glaciers at the end of the Little Ice Age and in recent years have defined the extent of the glacier fore-fields. In addition, a digital terrain model contributed information about the elevation. Vegetation was examined using the Normalised Difference Vegetation Index, calculated from the optical satellite data. A threshold classification on this vegetation index was used to track the extents of primary and already further developed vegetation. Following glacier retreat, most glaciers show considerable growth of primary vegetation starting within the first 30 years, while the majority of developed vegetation grows after 100 to 150 years. Comparing the time span between the end of the Little Ice Age and 1990 to the last 30 years, a general effect of climate change can be detected on the scale of the Swiss Alps that improves growing conditions. Although the larger glacier fore-fields showed a decreasing expansion of primary vegetation, as most of the habitable area was already vegetated, they experienced an increase in the expansion of developed vegetation. As a trend, both primary and developed vegetation uphold their rate of expansion in higher elevated parts of the glacier fore-field.

Table of Contents

1. Introduction

The evolution of glaciers since the end of the Little Ice Age (LIA) in the middle of the 19th century is marked by phases of retreat with smaller periods of glacier advances in various regions of the world (Grove, 2013; Paul and Bolch, 2019). There are evidences in the European Alps (Hagg et al., 2012), the Pyrenees (Cía et al., 2005; Marti et al., 2015), Scandinavia (Berdwell et al., 2008; Hannesdóttir et al.), the American (Hall and Fagre, 2003) as well as the Canadian (Luckman, 2000) Rockies, and the tropical Andes (Rabatel et al., 2008). The timing of the end of the LIA differs slightly around the globe, but in the European Alps, this was around 1850 (Grove, 2013; Rabatel et al., 2008). Glacier retreat increased in most of these regions during the most recent years (Paul and Bolch, 2019). As glaciers melt and, in the case of many small ones, vanish, new land is steadily replacing the previously glaciated areas. This newly exposed area builds up the glacier fore-field.

The glacier fore-field, in the following also referred to as the pro-glacial area, is not a static desert (Jochimsen, 1962), but rather a dynamic place marked by the development of new soils and plant succession at various speeds (Egli et al., 2011; Eichel, 2019). The surface cover changes from glacier ice to a mosaic of rock, sediments, vegetation and water, all with different effects on the local energy balance (Duveiller et al., 2018; Montague and Kjelgren, 2004). Further, these changes, together with the parent material below the surface, affect hydrological processes on the glacier fore-field (Magnusson, 2012; Tresch, 2007). After glacier retreat, the frequency of sediment movements such as debris flows increases (Haeberli, 1995). Such movements also affect the development of soils and vegetation, but when plant biomass is large enough, vegetation starts stabilizing the glacier sediments and thus facilitates the growth of further vegetation (Eichel, 2019). With vegetation being tied to hydrological, morphological, radiative and soil conditions, the observation of vegetation on the glacier fore-field allows drawing conclusions on the site-specific conditions. Their recent history and state allow vegetation growth at least to the observed degree and are, in particular in the case of soil and morphology, in turn influenced by the vegetation cover.

There are many studies about vegetation succession on glacier fore-fields, but most of them investigate only one or few pro-glacial areas. However, there are some studies on a regional scale. Schumann et al. (2016) analysed vegetation succession on 16 glaciers fore-fields within the Alps and Robbins and Matthews (2018) studied the variability of vascular plant species composition on 39 glacier fore-fields in Norway. However, these studies still rely on field campaigns. Meta analyses are one possibility for a larger scale overview, but studies about smaller and remote glaciers are scarce in comparison to the larger, more prominent glaciers. Still, glaciers in the Swiss Alps are frequently monitored thanks to organizations such as the Glacier Monitoring Switzerland (GLAMOS) or projects such as the Swiss Glacier Inventory (SGI, e.g. Paul et al., 2002). Further studies analysed the temporal evolution of digital elevation models (DEMs) such as Weidmann et al. (2019) or mapped historical glacier outlines (Freudiger et al., 2018). Several of these projects produced glacier extents of different times in a digital format. Combined with data from the Landsat satellite series which started in 1972, these data sets offer the potential to analyse the vegetation dynamics on all of the Swiss glacier fore-fields with a time series of optical satellite data with a length of at maximum 46 years (state 2018).

The digitalized glacier outlines from the end of the LIA, 1973 (Maisch, 2000) and 2010 (Fischer et al., 2014) are available in the form of shapefiles and contain the geocoded location and extent of the glaciers in Switzerland. The extent of the glacier retreat area since the end of the LIA marks the pro-glacial area since that has grown since 1850. The proximity to the different glacier outlines gives an indication of the duration for which an area has been ice-free with respect to a reference year. In this work, this duration is referred to as "terrain age" and the reference year the terrain age is calculated to is 2010. Additionally, the shapefiles allow an automated extraction of information about the glacier fore-fields from the satellite data or a DEM.

A common means to identify the extent of vegetation in an optical satellite image is the Normalised Difference Vegetation Index (NDVI). Apart from tracking the extent of vegetation, the NDVI has further merits over the use of raw satellite-derived reflectance. The NDVI shows a relatively low sensitivity to variations in soil background and illumination conditions (Myneni and Asrar, 1994) . The NDVI was also found to be less sensitive to topographic effects than other vegetation indexes such as the Enhanced Vegetation Index (Galvão et al., 2016; Matsushita et al., 2007), even though, there still is an effect (Teillet and Staenz, 2014). According to Song et al. (2001), classification and change detection using NDVI requires, if at all, only a simple atmospheric correction. These merits contribute to the popularity of the NDVI as a mean to study vegetation dynamics.

The NDVI has already been successfully used to characterize vegetation changes in various contexts such as the Swedish mountain ranges (Nordberg and Evertson, 2005), the Yangtze river delta (Zhao et al., 2009), drained lake basins in Alaska (Regmi et al., 2012), the Arctic Tundra (Stow et al., 2004) and also single pro-glacial areas (Walker et al., 1995). However, none of these studies has so far systematically analysed vegetation dynamics within glacier fore-fields on the scale of a larger region. In the intent to star filling this gap, the following research questions arise:

1. Can vegetation be detected, and can its extent be quantified in the fore-fields of Swiss glaciers using 30 years of optical satellite data?
2. At what terrain age can the presence of primary and developed vegetation be detected on the scale of the Swiss Alps?
3. How has vegetation cover changed from 1850 to 1973/1985 compared to the last 30 years?
4. Are trends in vegetation growth consistent across the Switzerland when considering the impacts of elevation and size of the glacier fore-fields?

To approach these questions, a test site was chosen and used to develop the basis of this analysis. In a second step, the investigation was scaled up to cover all the Swiss glacier fore-fields. The approach combines satellite-derived NDVI data with the digitalized glacier extent at different times and the digital terrain model of the glacier fore-fields.

2. Study region and data sets

2.1 Swiss glaciers fore-fields

The Swiss glaciers had their last integral maximum extent at the end of the LIA, a phenomenon that occurred roughly between 1300 and 1850 (Paul and Bolch, 2019; Wanner et al., 2008). During the LIA, the weather was not continuously cold, but rather variable as today (Grove, 2013). However, weather conditions that favour glacier advance such as wet winters and cold summers were more frequent and more aggregated around the globe (Grove, 2013). These climatic conditions of the LIA were likely caused by a combination of lower solar activity, lower summer insolation due to orbital forcing, and the considerable eruptions of several tropical volcanos (Wanner et al., 2008). During the LIA, the extents of the glaciers were not monotonously increasing but experienced several phases of advance and retreat (Grove, 2013). As markers from this climate anomaly, lateral moraines of the former glacier extent at the end of the LIA allow recreating and digitalizing past glacier extents in the field using topographic data, satellite images or aerial photography (Fischer et al., 2014; Maisch, 2000).

The retreat of the Swiss glaciers since the end of the LIA was also not linear. There were periods of colder and warmer years with more or less winter precipitation, resulting in fluctuations of glacier termini depending on how quick the glaciers adapt to such changes (response times). Figure 1 from Vaughan et al. (2013) shows stagnation of the retreat or even advances for glaciers with shorter response times around 1890, in the 1920s and during the 1970s and 1980s (Grove, 2013; Paul and Bolch, 2019). For the largest glaciers, cumulative retreats of about 1 – 2.5 km since the LIA have been observed (e.g. Great Aletsch, Gorner) whereas some glaciers with short response times advanced several hundred meters (e.g. Trient).

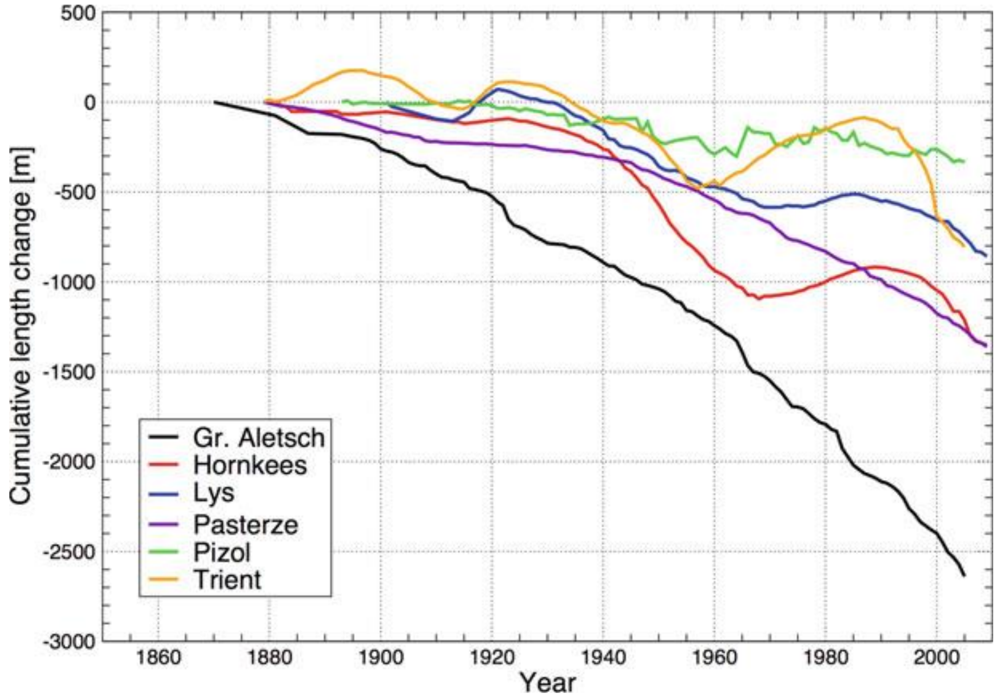

Figure 1: Evolution of cumulative glacier length changes in central Europe between the LIA and the early years of the 21st century shown for selected glaciers (sources: WGMS, http://www.climatechange2013.org/report/reports-graphic/ch4-graphics/, Vaughan et al., 2013).

Apart from variations in the glacier length, the area of the Alps being covered by glaciers was also reduced. Studies focussing on the change of glacier surface found areal losses of 30-40% between 1850 and 1970, resulting in an areal loss rate of 0.3% year^{-1}, and further 15-20% loss between 1973 and 2000, resulting in an increased loss rate of 0.6% year^{-1}, and additional 10-15% area loss between 2000 and 2010, resulting in a rate of 1.2% year^{-1}. In total, an area loss of 50-60% over the entire period of 1850 to 2010 has been observed (Fischer et al., 2014, 2015; Maisch, 2000; Paul and Bolch, 2019; Zemp et al., 2008). According to Carrivick et al. (2019), Swiss glacier fore-fields in 2010 had a combined area of about 600 km^2 and were attributed to about 2170 individual pro-glacial areas of which 60% were still connected to glaciers in 2010 while 40% were at their maximum size as their corresponding glaciers had completely disappeared. Analysis of the distribution of elevation across the pro-glacial areas by Carrivick et al. (2019) found most glacier fore-fields to be close to a uniform distribution of area with altitude. All this area converted from glaciers to glacier fore-fields is, as stated by Jochimsen (1962), not just barren land. Over time, the pro-glacial area gets colonised by plants, which starts the formation of soils and these soils in turn allow the growth of further vegetation (Eichel, 2019; Temme, 2019).

The development of soils on Swiss glacier fore-fields was studied by Temme (2019), who found that, over all, the most important factor on rates of soil development was the age of the exposed area. After a slow start with low values in the first few years after the glacier retreat, the rates mostly show increases reaching a maximum for ages between 100 and 1000 years (Temme, 2019). However, other factors than terrain age can have distinct impacts on soil development rates such as the geology of the parent material, climatic differences between the pro-glacial areas, different morpho-dynamical settings and vegetation succession (Temme, 2019). The interaction with vegetation is two sided. On the one hand, vegetation provides material to build up the soil, on the other hand, the diversity of the soils present in the glacier fore-field determines biodiversity, as different soils enable the growth of different plant communities (Temme, 2019).

At the start of vegetation succession, physical properties are driving vegetation growth (Eichel, 2019). Soil development and temperature increase improve conditions for vegetation, resulting in relatively quick succession rates until a terrain age of about 50 years (Matthews, 1992). Eichel (2019) divided vegetation succession into four segments. In the pioneer stage (terrain age of 0 – 15 years), the pro-glacial area is colonized within a few years (Matthews, 1992; Nagl and Erschbamer, 2010), in some cases even within one year (Cannone et al., 2008). However, the mortality of seedlings and plants is still high (Marcante et al., 2009) and vegetation cover is on a low (< 10%) level (Nagl and Erschbamer, 2010). The early-successional stage (terrain age of ~ 15-40 years) is characterized by improved environmental conditions through advanced soil development, a more stable substrate and higher temperatures (Matthews and Vater, 2015). The vegetation cover can reach 30 – 50% and the vegetation community diversifies (Matthews, 1992; Raffl et al., 2006). During the intermediate successional stage (terrain age of ~40 – 80 years) first shrubs appear (Raffl et al., 2006). Vegetation cover increases further (around 60 – 70%) and species diversity reaches its maximum (Ellenberg and Leuschner, 2010). In the late-successional stage (terrain age above 80 – 100 years), the first trees appear in areas below the timberline and the plant community shifts from pioneer to more competitive species (Marcante et al., 2009). During vegetation succession, the increasing amount of plant biomass starts affecting geomorphic processes which stabilizes the glacial sediments, facilitating further plant succession (Eichel, 2019).

This study aims to analyse vegetation dynamics on the scale of the glacier fore-fields within the Swiss Alps, but in order to develop the approach and serve as an example site to demonstrate results, a test site was chosen. This pro-glacial area needed to be large enough and contain enough vegetation to show distinct changes. Additionally, field studies of this glacier fore-field and a vegetation map enable a deeper discussion of the results of this specific area. The glacier fore-field of the Morteratsch glacier satisfies these requirements well. Especially the availability of literature is of advantage. A photographic impression of the vegetation succession in the Morteratsch glacier fore-field can be found on the swisseduc website (swisseduc.ch, see Figure 2) There is even a glacier trail providing information about several aspects of the glacier and its fore-field (Maisch et al., 1993).

Figure 2: Images of the Morteratsch glacier fore-field at the frontal position of the glacier in 1960, taken in 1985 (a) and 2002 (b), source: swisseduc.ch.

2.2 Morteratsch glacier fore-field

The fore-field of the Morteratsch glacier is located in the Upper Engadin. Near the glacier tongue, the distance between the glacier (as of 2010) and the end of the glacier fore-field is about 2.5 km and the altitude ranges from about 1900 to 2200 m a.s.l. Some parts that are already ice-free but located above the glacier tongue are even above 3000 m a.s.l. The total pro-glacial area measures about 4 km^2. The glacier itself is within the Swiss glaciers rather long and therefore its length reacts rather slow to environmental changes (Maisch et al., 1993).

Since the LIA, summer temperatures in the area of the Morteratsch glacier increased by 1 – 1.5 °C (Zekollari et al., 2014). This caused a retreat of the glacier of on average about 16 m/year since the LIA, with phases of slower retreat between 1900 and 1920 as well as in the later 1960s and a faster retreat between 1935 and 1965 (Maisch et al., 1993), as also illustrated in Figure 3. The silicate substrate in the fore-field is rather acidic (pH of ~ 6) and in the area 50-100 m around the glacier mostly free from vegetation (Maisch et al., 1993). First flowering plants occur after a terrain age of 5 – 8 years, first grasses on areas that are ice-free for 8-10 years (about 200 m distance to the glacier) and even though some smaller larches grow closer to the glacier, woody plants grow preferred in the lowest part of the pro-glacial area (Maisch et al., 1993). In the area surrounding the glacier fore-field, the forest boundary is located at about 2200 to 2350 m a.s.l. A vegetation map from the Morteratsch glacier fore-field (Burga et al., 2010) is shown in Figure 4. The map also shows the position of the glacier tongue in several years between 1857 and 1997.

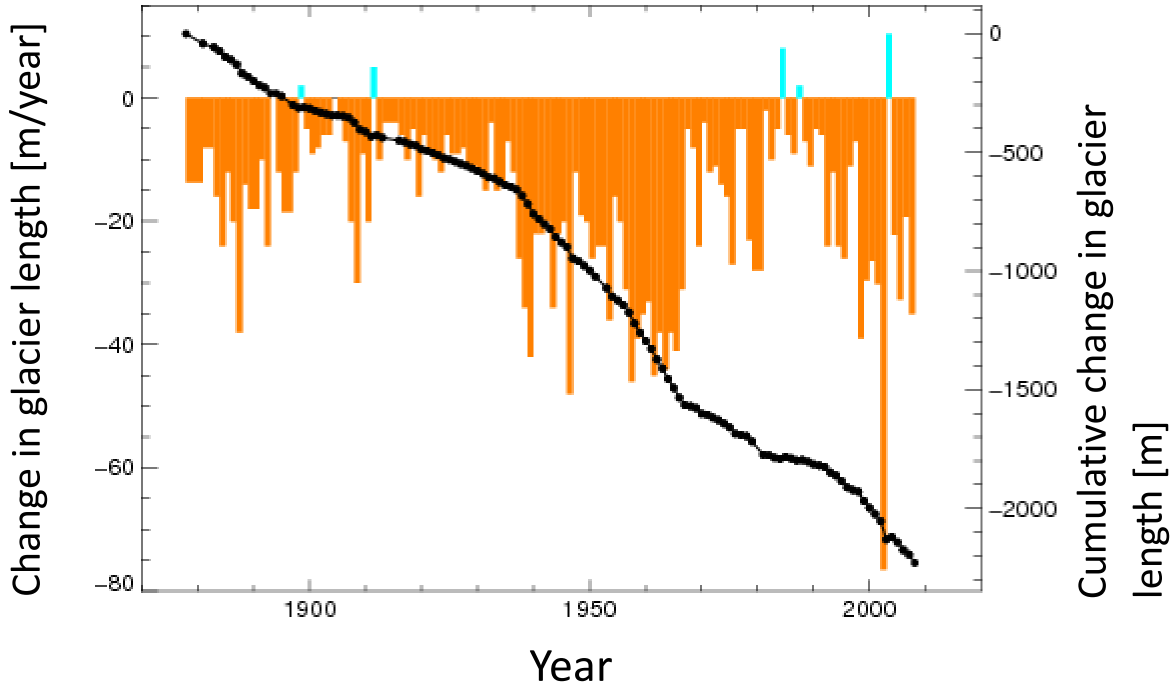

Figure 3: Plot of the change in glacier length and cumulative change in glacier length for the Morteratsch glacier since the end of the LIA. Source: gletscherg2g.wordpress.com.

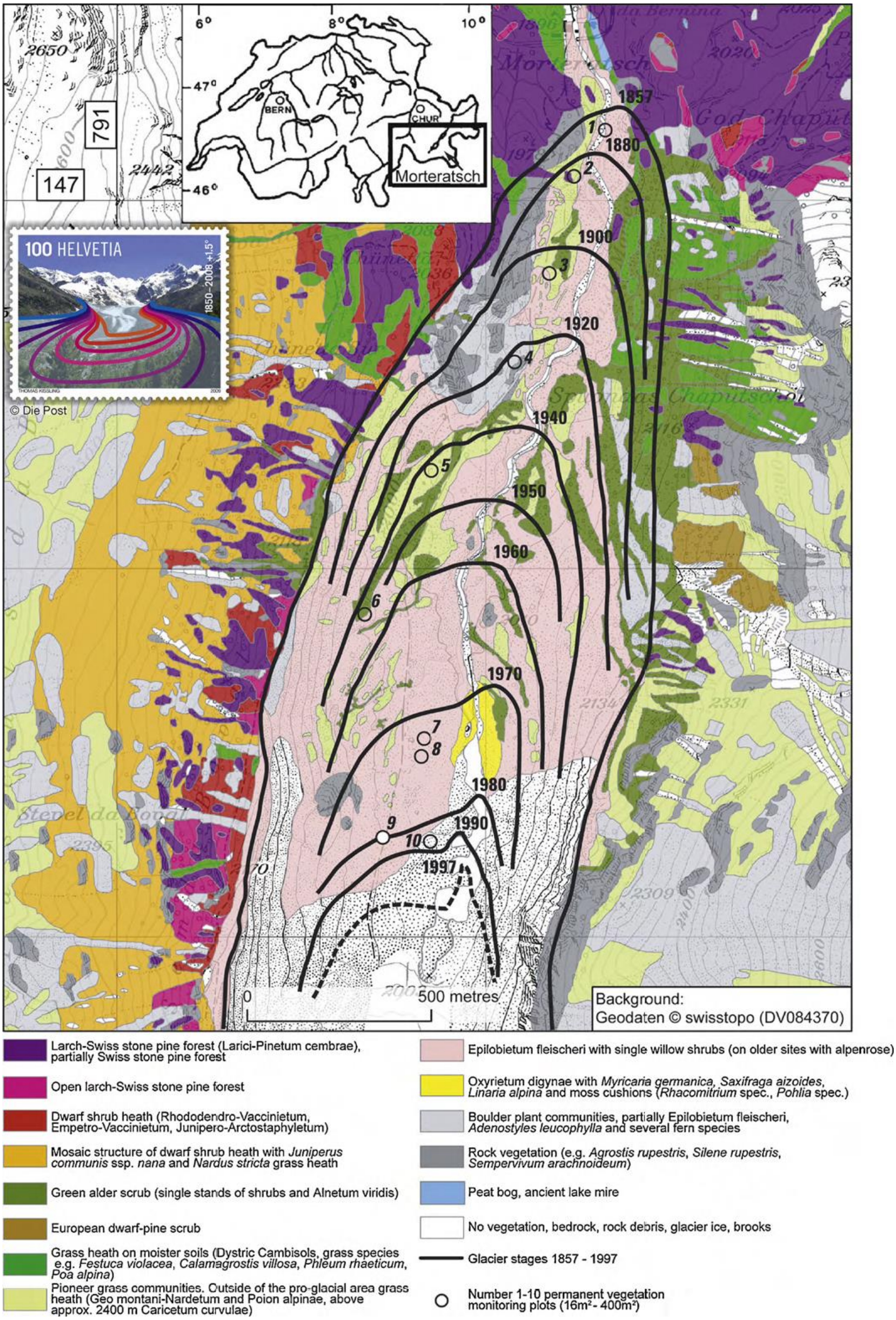

Figure 4: Vegetation map of the tip of the Morteratsch pro-glacial area modified and completed after (Fischer, 1999). The black lines indicate the position of the end of the glacier between 1857 and 1997 after (Burga, 1999). Source: (Burga et al., 2010).

2.4 Data sets

For the Swiss glaciers, shapefiles with the extent and position of the glaciers of 2010 (inventory from M. Fischer), around 1973 and at the end of the LIA are available (Fischer et al., 2014; Maisch, 2000). The change between the states of 2010 and the LIA defines the glacier forefield. The swissALTI3D DEM of Switzerland (Swisstopo, 2018) was used to derive information about altitude and hillslope in the pro-glacial areas of the Swiss Alps. The Landsat series are a collaboration of the National Aeronautics and Space Administration (NASA) and the United States Geological Survey (USGS), aimed at measuring Earth's terrestrial and polar surfaces in a repeat cycle of about 16 days per satellite (Roy et al., 2014). The timeline of the Landsat satellite missions is shown in Appendix 1.

Optical satellite images cover a certain range of wavelengths and can be used to distinguish land cover types with different spectral behaviour, as illustrated in Figure 5. The spectral bands of Landsat 7 and 8 are illustrated in Figure 6. Tables with the instruments of Landsat 5, 7 and 8 indicating their band specifications can be found in Appendix 2 and Appendix 3. Scenes from Landsat 5, 7 and 8 (source: USGS archives, accessed through the Google Earth Engine (GEE), https://code.earthengine.google.com/) provide the time series of satellite images from 1984 to 2017. The images have a spatial resolution of 30 m. Images from the visible and Near-Infrared (VNIR) spectral regions were used, even though the Landsat series included further spectral bands, as shown in Figure 6 and Appendix 2. The consistency of spectral (Flood, 2014; Teillet et al., 2001) and NDVI (Roy et al., 2016; Vogelmann et al., 2001) data from the different Landsat missions has been tested and differences are small enough for the chosen applications. In this thesis, the images of the Swiss Alps acquired from Landsat 5, 7 and 8 were combined to a time series of 34 years (1984 – 2017).

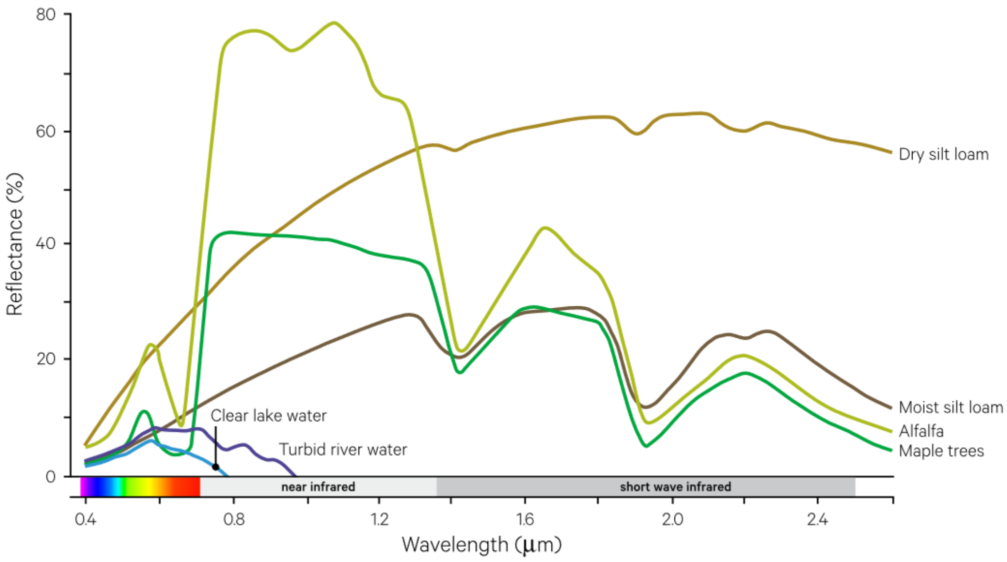

Figure 5: Spectra of different land cover classes in reflectance (%) for different wavelengths (μm) of incoming radiation (Harrison and Jupp, 1989).

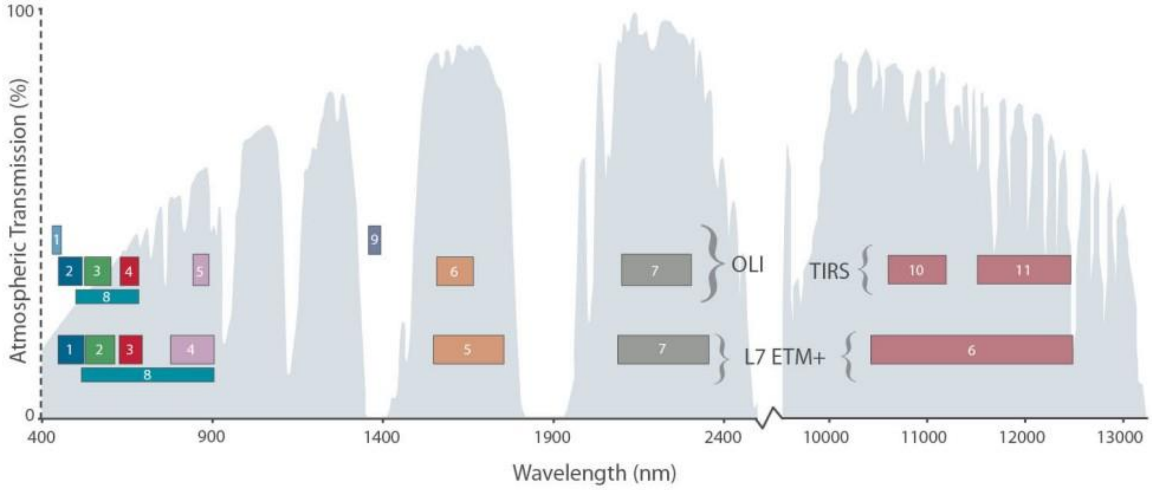

Figure 6: Comparison of the Operational Land Imager (OLI) bands of Landsat 8 and the Enhanced Thematic Mapper Plus (ETM+) bands of Landsat 7. The Thermal instrument (TIRS) adds two thermal infrared bands to Landsat 8 (source: landsat.gsfc.nasa.gov)

The vegetation map of the Morteratsch glacier fore-field from (Burga et al., 2010), shown in Figure 4, was used to relate the results from the satellite data to vegetation occurrence, at least for Morteratsch. Figure 4 also shows the position of the glacier tongue in intervals of 20 years. The map is based on field observations by (Fischer, 1999) which were extended and completed by (Burga et al., 2010).

3. Methods

3.1 Data preparation

The Landsat data was processed in the GEE to derive vegetation presence in pro-glacial areas. Within a year, all scenes from 1st of April to the 1st of October combined to an image collection. Landsat 5 data was used for the years 1984 – 2000, Landsat 7 for 2001 – 2012 and Landsat 8 for 2013 – 2017. The extent of the scenes was chosen to range from 45.6319° N to 47.8854° N and from 5.9026° E to 10.9818° E (WGS 84) and thus equal to the extent of the shape files of the glaciers' positions. The shapefiles of the glacier extents in 1850, 1973 and 2010 were used to locate the glacier fore-fields (see Figure 7, a). The scene taken at the 9th of June 2017 by the Landsat 8 satellite are displayed in Figure 7 (b) as RGB image and in Figure 7 (c) as false colour image (NIR-red-green) as an example of a single scene image and for orientation.

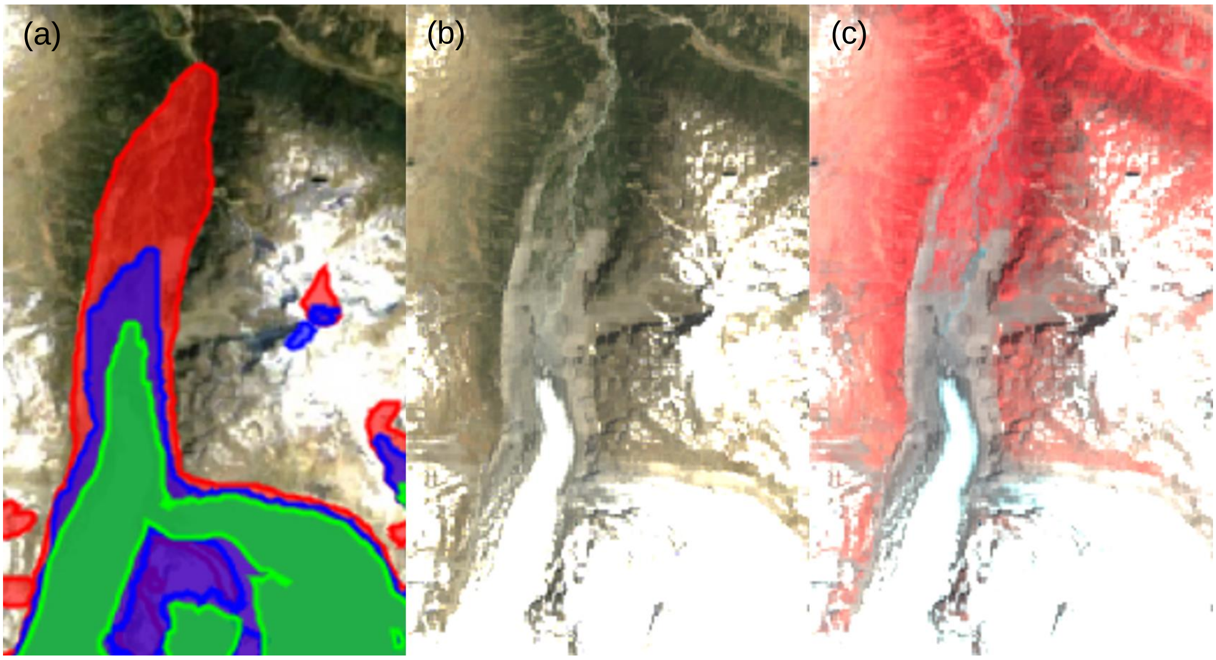

Figure 7: Shapefiles of the glacier extent in 1850 (red), 1973 (blue) and 2010 (green) in the region of the Morteratsch glacier (a). RGB image (b), and false colour image (NIR-red-green, c) of the Morteratsch area, taken by Landsat 8 at the 9th of June 2017.

From the available bands shown in the images in Figure 7 (b and c), only the red (Figure 8, a) and NIR (Figure 8, b) cannel were used for the further evaluation. To obtain an index of vegetation presence in the Landsat scene, the NDVI was calculated according to Equation 1. The NDVI for the scene of the 9th of June 2017 is displayed in Figure 8 (c) as an example. This calculation was performed for every scene in the evaluation.

$$NDVI = \frac{NIR - Red}{NIR + Red} \quad (1)$$

Equation 1: Calculation of the NDVI using the Near Infrared (NIR) and red band. The red band for Landsat 8 is defined between 0.64 and 0.67 µm and the NIR band between 0.85 and 0.88 µm.

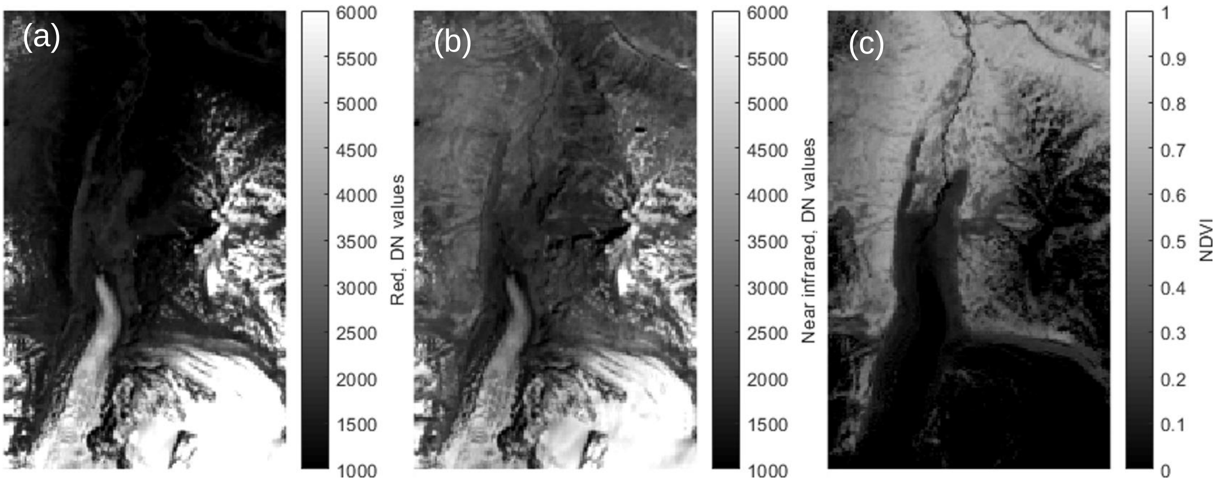

Figure 8: Red (a) and Near Infrared (b) channel of the Morteratsch area shown in digital numbers (DN), taken by Landsat 8 at the 9th of June 2017. The NDVI (c) was calculated from the red (a) and Near Infrared (b) channels.

This resulted in several NDVI scenes per year (32 in the example of the Morteratsch area in 2017 as shown in Figure 9; total number of scenes for the Swiss Alps in 2017: 184 scenes). As visible in Figure 9, there are several single scenes with missing information, as there was only a fraction of the image part of the measured area or due to cloud cover. Clouds show a high reflectance in both red and NIR, as visible in Figure 8. Thus, cloud covered pixels have a low NDVI regardless of what land cover type is obscured by the cloud. Some might also contain artefacts of too high values, as the image second from right in the top row. Following Equation (1), NDVI is highest where the difference of NIR and red is closest to their sum. In the case of vegetation, NIR is strongly reflected and red is absorbed, as shown in Figure 5, causing the high NDVI. Another possibility to get high NDVI values are NIR and red values close to 0. Thus, the difference is small, but normalized with a small sum, causing a false positive in vegetation detection. Within a year, NDVI varies with vegetation activity, which affects both the high NIR reflection and the absorption of the red spectrum.

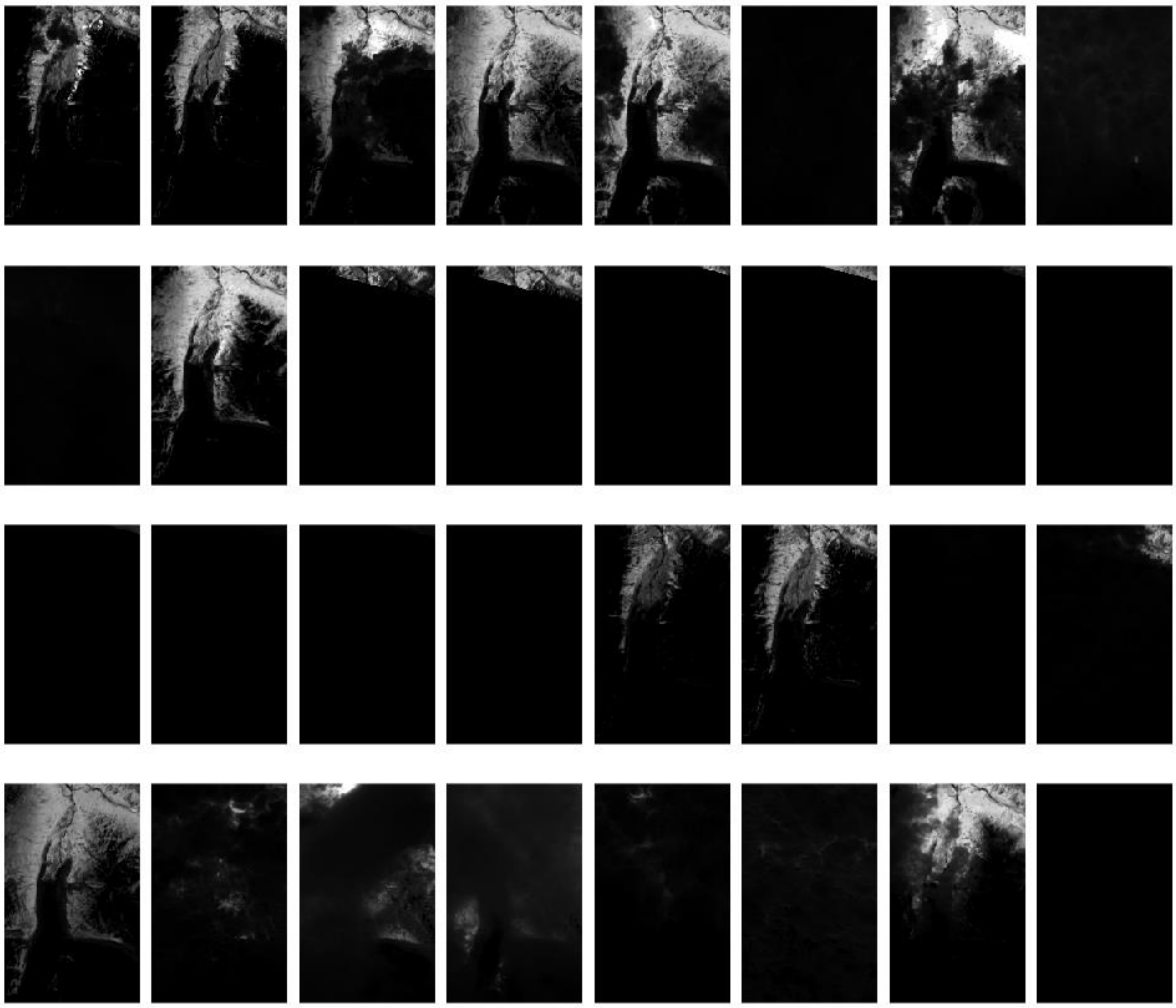

Figure 9: Set of 32 single NDVI scenes of the Morteratsch region acquired by Landsat 8 between 1st of April and the 1st of October 2017.

To get information about vegetation presence alone, the evolution of NDVI during the year is less important. The idea is to extract the highest NDVI-value per pixel and per year, but as far as possible with the exclusion of artefacts. Thus, in order to get a single, representative NDVI map for each year between 1984 and 2017, the 95-percentile value from all NDVI values of every pixel on the scene was extracted. Figure 10 (a) shows the composite of the 95-percentile values of the scenes from 2017 with a zoom-in on the lower end of the pro-glacial area of the year 2000 in Figure 10 (b).

As the Landsat data has a spatial resolution of 30 m, it is assumed that different land cover classes contribute to the NDVI value of a pixel. For the glacier fore-field, the assumption was made that the maximum NDVI value of a year correlates with the density of vegetation within the observed pixel. Even tough an individual plant possesses spectral properties leading to a high NDVI, the value is lower on a 30 m pixel on with only a small contributes of vegetation to the pixel area.

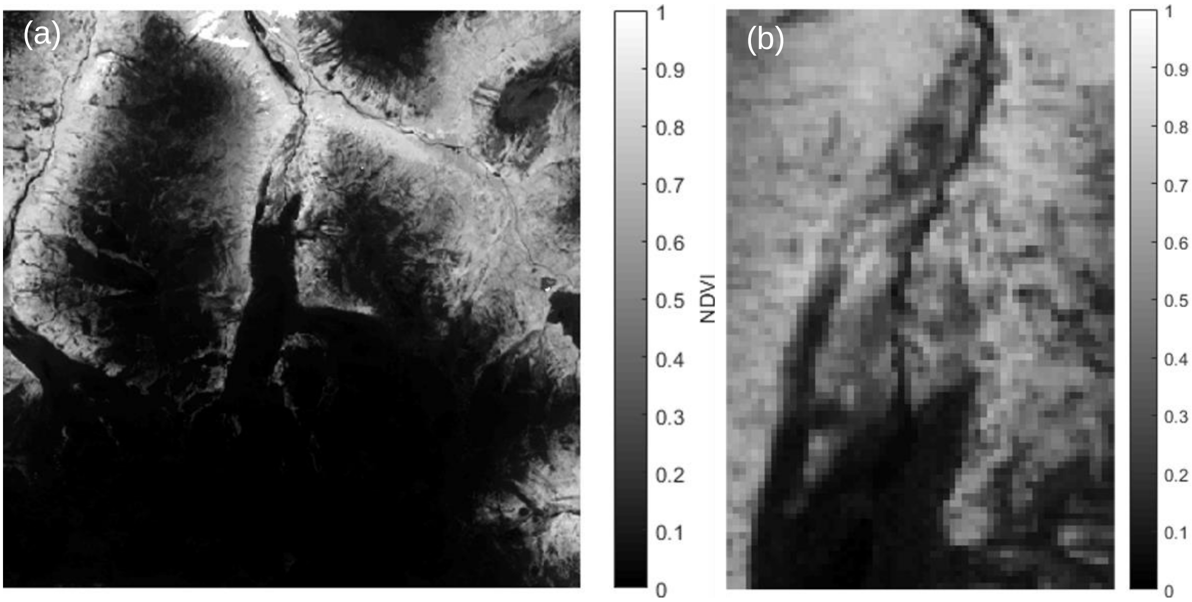

Figure 10: (a): The NDVI of the Morteratsch area in the year 2017 composed of the 95-percentlie NDVI values. (b): Vegetation Index at the tip of the Morteratsch pro-glacial area in the year 2000 composed of the 95-percentlie NDVI values.

The step of calculating the 95-percentile NDVI composite was performed using the GEE, as it allowed calculating the NDVI maps of all considered single scenes and extracting the 95-percentile values per year on the GEE-servers without downloading each individual scene. Thus, only one dataset per year containing for every pixel the 95-percentile NDVI value within the extent specified at the start of this chapter was downloaded.

The extents of primary and developed vegetation cover were obtained from NDVI maps by applying a binary threshold classification. All pixels with NDVI being lower than 0.2 were considered no vegetation and all pixels equal to or above the threshold value are classified as vegetation. Pixels with NDVI of at least 0.2 were classified as vegetation including primary vegetation and areas with higher vegetation cover, while the extent of already developed vegetation cover was tracked using a higher threshold value of 0.6. The extent of primary vegetation in 2017 is illustrated in Figure 11 (a) and of developed vegetation in Figure 11 (b). The workflow used to derive the NDVI composite and the classification of primary and developed vegetation is shown in Figure 12 for illustration. Accordingly, growth of primary vegetation within a pixel was detected when NDVI values changed from below 0.2 to above 0.2 and analogously for developed vegetation with the NDVI increasing above 0.6.

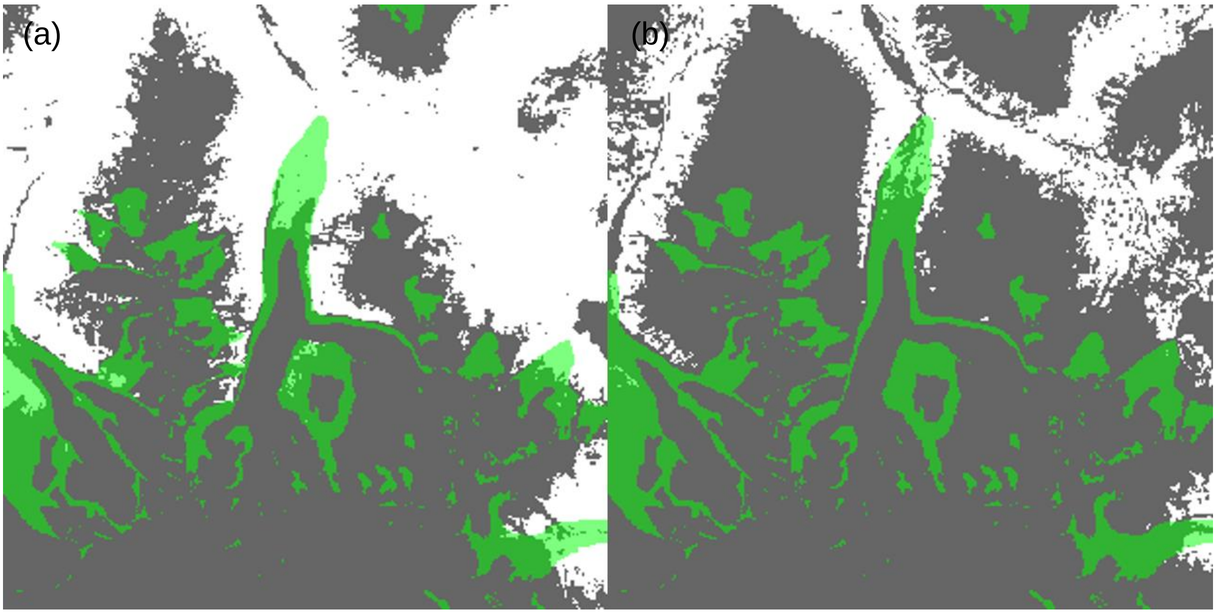

Figure 11: Extent of vegetation of primary (a) and developed (b) succession stage in 2017 based on the binary classification of the NDVI values displayed in Figure 10 (a). White areas were classified as vegetated and dark grey areas as not vegetated. The extent of the glacier fore-fields is overlain in green. The used classification thresholds were 0.2 (a) and 0.6 (b).

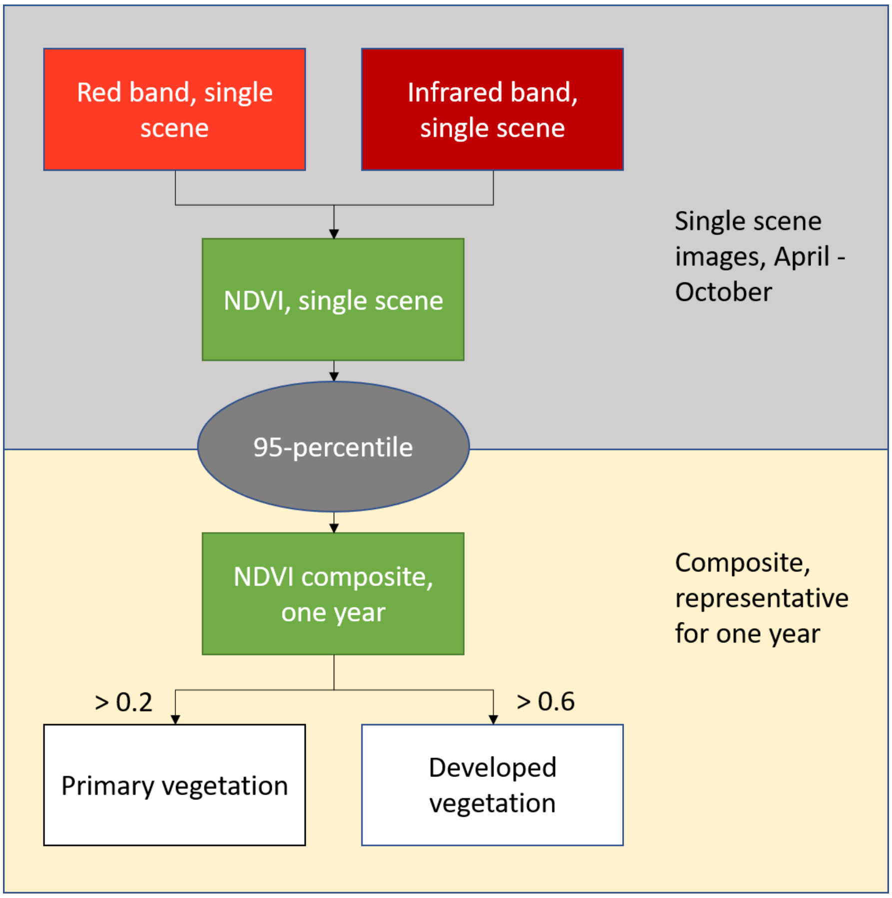

Figure 12: Illustration of the workflow applied to every year covered in the analysis in order to derive NDVI composite images and the classification of primary and developed vegetation from red and NIR scenes of the single scenes of the respective year.

Additional information about the glacier fore-fields was calculated from the swissALTI3d topographic model after resampling from 5 m to 30 m to match the spatial resolution of the satellite data. The topographic model also contained the hillshade which displayed in Figure 13 together with elevation. The topography data was also clipped with the shapefile of the glacier fore-fields. For every pro-glacial area, the size was calculated from the number of pixels contained in the glacier fore-field with one pixel having a size of 900 m^2.

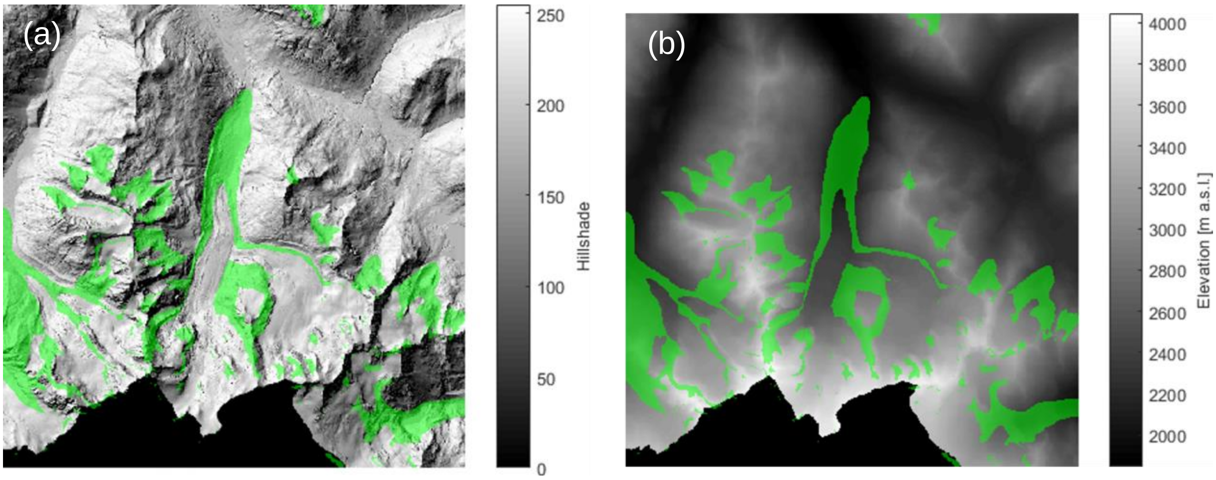

Figure 13: : Section of the digital terrain model from SwissALTI3d (Swisstopo, 2018) showing hillshade (a) and elevation in m a.s.l. (b) in the area of the Morteratsch glacier fore-field. The pro-glacial area is indicated in green.

The shapes of the glacier extents in 1850, 1973 and 2010 from (Maisch, 2000; Fischer et al., 2014) were used to fit a surface between those borders to get an estimate of terrain age for every pixel on the pro-glacial area, as illustrated in Figure 14. The surface fit was performed using the gridfit function from John R. D'Errico (as of December 2016). With the extent of the glaciers in 2010 closing the area of the glacier fore-fields, 2010 was chosen as the reference year for the terrain age. Thus, terrain age on the pro-glacial area varies between 0 and 160 years. Compared to the positions of the tip of the Morteratsch glacier in Figure 4, the age interpolation resulted in a glacier retreat that was faster at the tip of the glacier fore-field. Further, the transition from the terrain age of about 110 years (dark green) to a terrain age of about 50 years (light green) in Figure 14 is more abrupt. All data about the pro-glacial areas were assembled in Matlab and provided the database for the analyses presented in the next sections. The information provided by the shapefiles was also used to assign an individual ID to each glacier fore-field in order to assemble information on the level of pro-glacial areas rather than on single pixels.

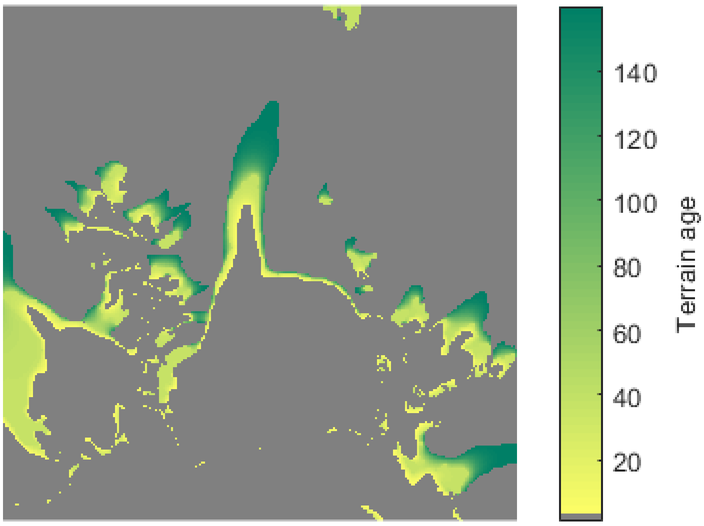

Figure 14: Terrain age in 2010 interpolated from the glacier extents of 1850, 1973 and 2010 from the 2010 glacier inventory from Mauro Fischer and from the Swiss Glacier Inventory (Maisch, 2000; Fischer et al., 2014).

To locate the glacier fore-fields on the Landsat and swissALTI3d data, the glacier extents from 1850 and 2010 were clipped to define the pro-glacial area between the extent of 1850 and 2010 (red and green in Figure ,7a). The shape of the pro-glacial areas was then used to extract the different values of the glacier fore-fields and assemble them in an organized data structure, which contains only the data of the glacier fore-fields. Figure 15 illustrates how the different components available for the entire scene were combined to the combined data set specific to the pro-glacial areas.

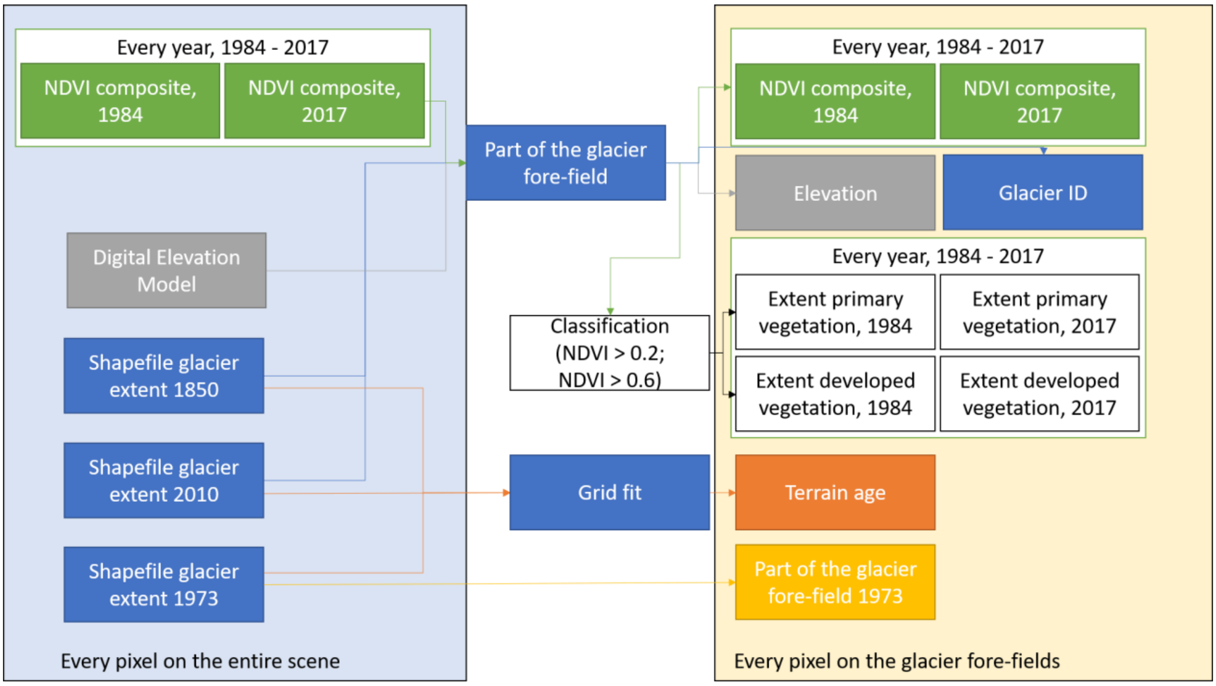

Figure 15: Workflow of the data preparation. The different datasets available for every pixel on the scene were combined to extract information only about the pixels which are part of a glacier fore-field.

3.2 Locating vegetation expansion

Changes in vegetation are tracked in two ways: First, as a difference in the NDVI values between points in space or time and second, as changes in a binary vegetation map. As a mean to compare different pro-glacial areas, the fraction of surface that was newly colonized by plants between 1990 and 2015 was calculated for every glacier fore-field. This was achieved in several steps, using a threshold value of 0.2 for primary vegetation classification and 0.6 on the NDVI data to classify developed vegetation succession. The following steps are illustrated in Figure 16.

- Start with the classification of the years 1987 - 1993 of every pixel in the pro-glacial area into vegetation or no vegetation.
- Derive the mode of the seven classification results for every pixel in the pro-glacial area to get the extent of vegetation at the beginning of the considered period.
- Continue with the classification of the years 2013 - 2017 and derive the mode of those five classification results for every pixel in the pro-glacial area to get the extent of vegetation at the end of the considered period.
- If both values are 0, the pixel is assumed to be without vegetation for the entire period.
- If both values are 1, the pixel is assumed to be continuously.
- The pixel was considered to have experienced vegetation expansion if the first mode was 0 and the second mode was 1.
- The pixel was considered to have experienced vegetation retreat if the first mode was 1 and the second mode was 0.
- The difference in the number of pixels considered to have experienced vegetation colonialization and retreat (expansion – retreat), divided by the number of pixels in the pro-glacial area for every pro-glacial area to get the relative area of vegetation expansion between 1990 and 2015.

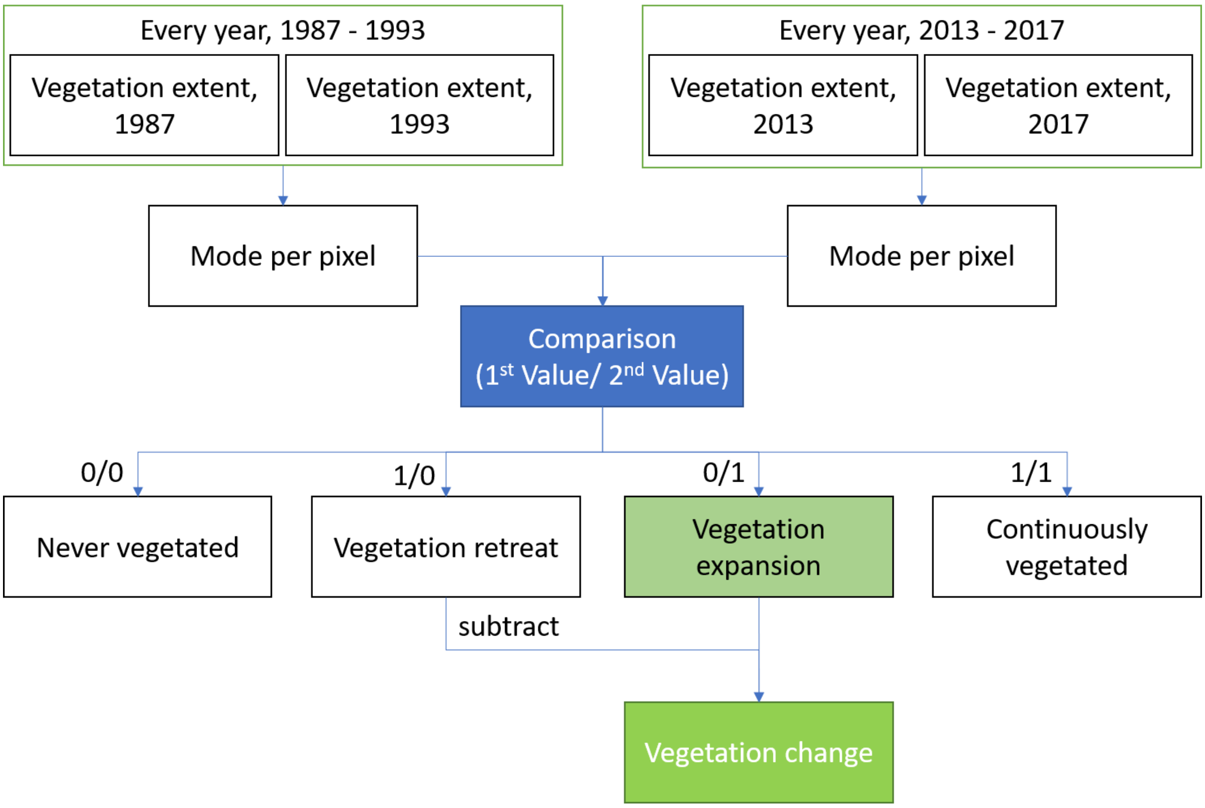

Figure 16: Workflow showing the processing of the annual NDVI-based vegetation classification data to assess the change in vegetation. The workflow was applied once for primary vegetation with a classification threshold of 0.2 on NDVI and once for developed vegetation using a threshold value of 0.6.

3.3 Temporal evolution of vegetation expansion

The information about where a change from non-vegetated area to vegetated area occurred was combined with the information about terrain age in the pro-glacial area to estimate the time between an area getting ice-free and the detection of primary or developed vegetation. The following procedure was performed once with a threshold value of 0.2 for the growth of primary vegetation and once with 0.6 for developed vegetation. The workflow as described in the following is illustrated in Figure 17.

- Start with the pixels that were found to have experienced vegetation expansion in the previous assessment. And determine for every pixel the year in which was it became ice-free by subtracting the terrain age from the reference year 2010.
- Classify all years of the pixels considered to have experienced vegetation colonialization by applying the vegetation threshold on the NDVI data.
- Extract the first year in which vegetation was classified and at which point at least 70% of the remaining years (including the considered year) are classified as vegetation. The colonialization is considered to have occurred in this year.
- The difference between the considered year of colonialization and the year in which the pixel was getting ice-free is considered to be the time required for vegetation succession of either primary (threshold 0.2) or developed vegetation (threshold 0.6).
- The years required for vegetation succession were arranged cumulatively in groups of 10 years for every glacier fore-field.
- Dividing the cumulative number of pixels in each group of 10 years by the number of pixels showing vegetation succession in the considered pro-glacial area achieved normalization.

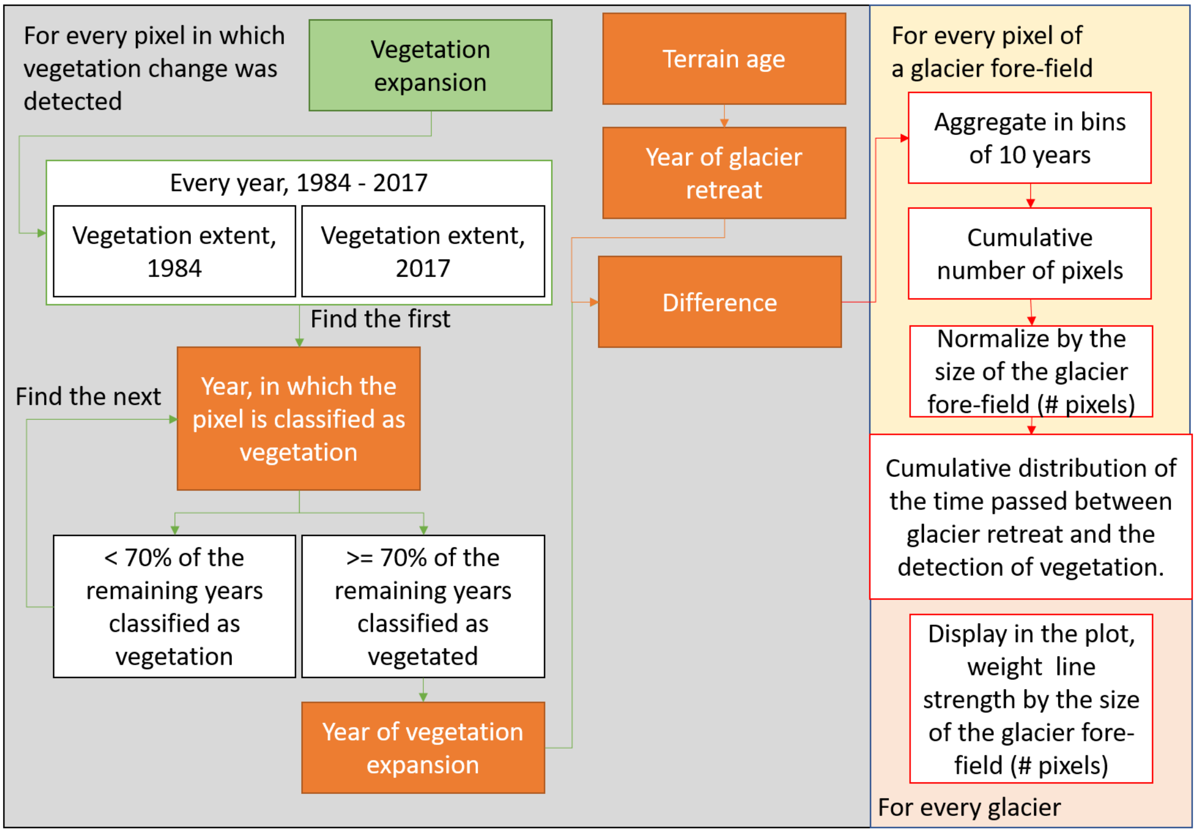

Figure 17: Based on the result of the workflow in Figure 16 (Vegetation expansion), this illustration shows how information about changes in vegetation were combined with the terrain age to approximate the distribution of the time passed between glacier retreat and the detection of vegetation. This was performed once for primary and once for developed vegetation.

The challenge of comparing vegetation dynamics in Swiss glacier fore-fields between the LIA and the 1980s to the last 30 years was approached by comparing rates of vegetation expansion. The considered time spans were 1850 – 1990 and 1850 – 2015. All the vegetation classified at the end of a time span was considered to have grown during this time span, as at the beginning (LIA glacier extent) no vegetation was present at all. After normalization for the size of the considered glacier fore-field and number of years in the respective time span, these rates resulted in the annual vegetation expansion as fraction of the extent of the pro-glacial area at the end of the time span. Subtracting the rate for the time 1850 – 1990 from the rate for 1850 – 2015 for every pro-glacial area served as an approach to compare the time 1990 – 2015 to 1850 – 1990. These rates and the difference in rates were calculated for both primary and developed vegetation, applying a classification threshold of 0.2 and 0.6, respectively. The workflow is illustrated in Figure 18.

- The classification threshold was applied on the NDVI values of the years 1987 - 1993 of each pro-glacial area.
- For each pixel, the mode of these five years is determined and used in the following.
- The number of pixels classified as vegetation is divided by the number of pixels in the glacier fore-field to get the relative area vegetated during the first time span.
- The relative vegetated area is divided by the number of years in the time span, being 140 years, resulting in the annual rate of vegetation expansion relative to the extent of the pro-glacial area. In the following, this is referred to as rate 1.
- The steps 1 to 4 are repeated as above using the NDVI values of the years 2013 – 2017 and a duration of the time span of 165 years. This second rate is in the following referred to as rate 2.
- Rate 1 is subtracted from rate 2 to get the difference in rates for every glacier fore-field.
- A one-sided student-t test was used to test whether the differences in rates of all the pro-glacial areas were higher than zero at the 5% significance level.

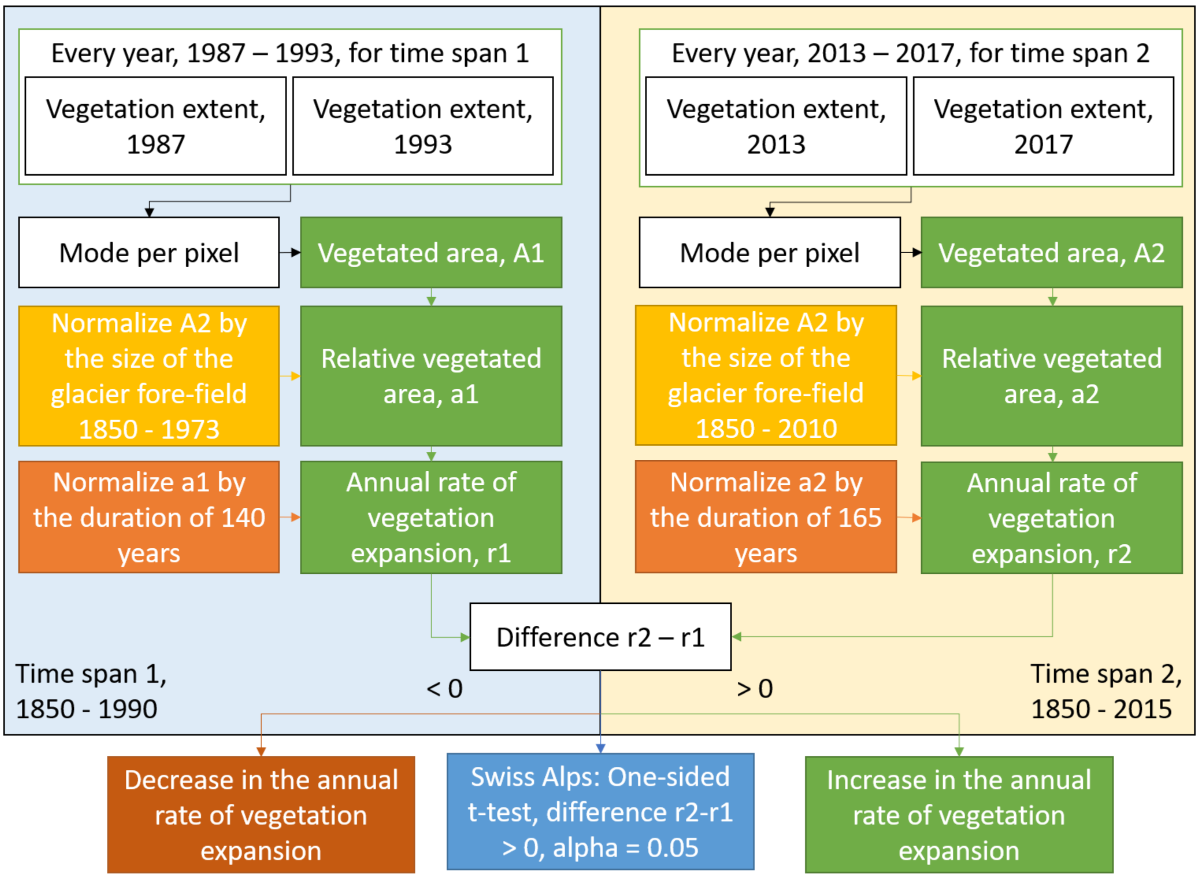

Figure 18: Workflow showing the calculation of the difference in the annual rate of vegetation expansion comparing vegetation expansion between 1850 and 1990 to the expansion between 1850 and 2015. This included a one-sided student-t-test to evaluate whether the differences of the total of glaciers in the Swiss Alps was significantly positive.

3.4 Comparison of results across geographic trends

The measures of vegetation dynamics described in the previous sections were also compared across glaciers and along geographic trends. Therefore, plots of the relative area of vegetation expansion between 1990 and 2015 and the difference in rates of vegetation expansion are shown in plots using the altitude and size of the pro-glacial area as additional information. As value for altitude, the mean altitude of all pixels in the respective pro-glacial area was used. The size of the pro-glacial are was calculated from the number of pixels in each respective pro-glacial area (900 m^2 per pixel). These plots show results on the scale of the Swiss Alps. As a map of the entire Swiss Alps showing the analysis of the pro-glacial areas in their spatial context is not suitable in the format of this document, results are first shown in the test region of the Morteratsch glacier and in a second step transferred to plots showing the results for all the glacier fore-fields within the Swiss Alps.

4. Results

4.1 Vegetation change

The changes in NDVI from 1989 to 2017 in the pro-glacial areas in the Morteratsch region are displayed in Figure 19. Generally, decreases in NDVI were found in the upper parts of the pro-glacial area and show amplitudes between 0 and 0.5 for most negative values. The increases are in general distinctly higher and occur rather in the lower, older part of the pro-glacial area, indicating that the density of vegetation has increased considerably. Most of the negative values are between 0 and -0.1. Some mostly isolated points show decreases in NDVI by 0.4 to 0.5 Increases reach values around 0.4 on larger areas such as the central part in the lowermost section of the Morteratsch glacier fore-field.

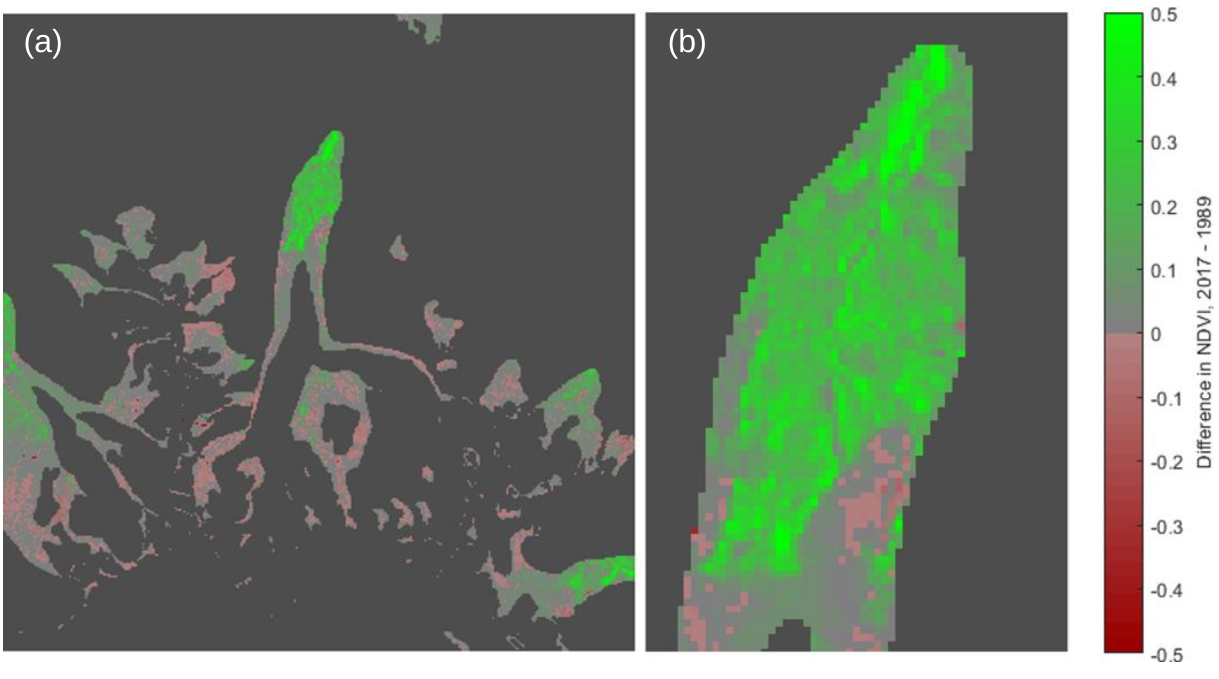

Figure 19: Change in NDVI from 1989 to 2017 calculated as the difference of the NDVI of 2017 minus the NDVI of 1989. The dark grey areas are outside of the pro-glacial areas.

Figure 20 shows the changes in the extent of primary vegetation in the Morteratsch region between 1989 and 2017. White areas were found to be vegetated in both 1989 and 2017 while dark grey areas were in neither of those years. Red areas were classified as vegetation in 1989 but no longer in 2017. There are some discontinuous, linear structures that fall into this category within otherwise dark areas. Otherwise, red areas are usually located in the transition zone between vegetation-free, dark areas and vegetated, white areas. The green areas had not been classified as vegetation in 1989 but fulfilled the criteria in 2017. Hence, these areas show an NDVI of at least 0.2. The tip of the Morteratsch glacier fore-field shows a considerable area assigned to vegetation expansion between 1989 and 2017.

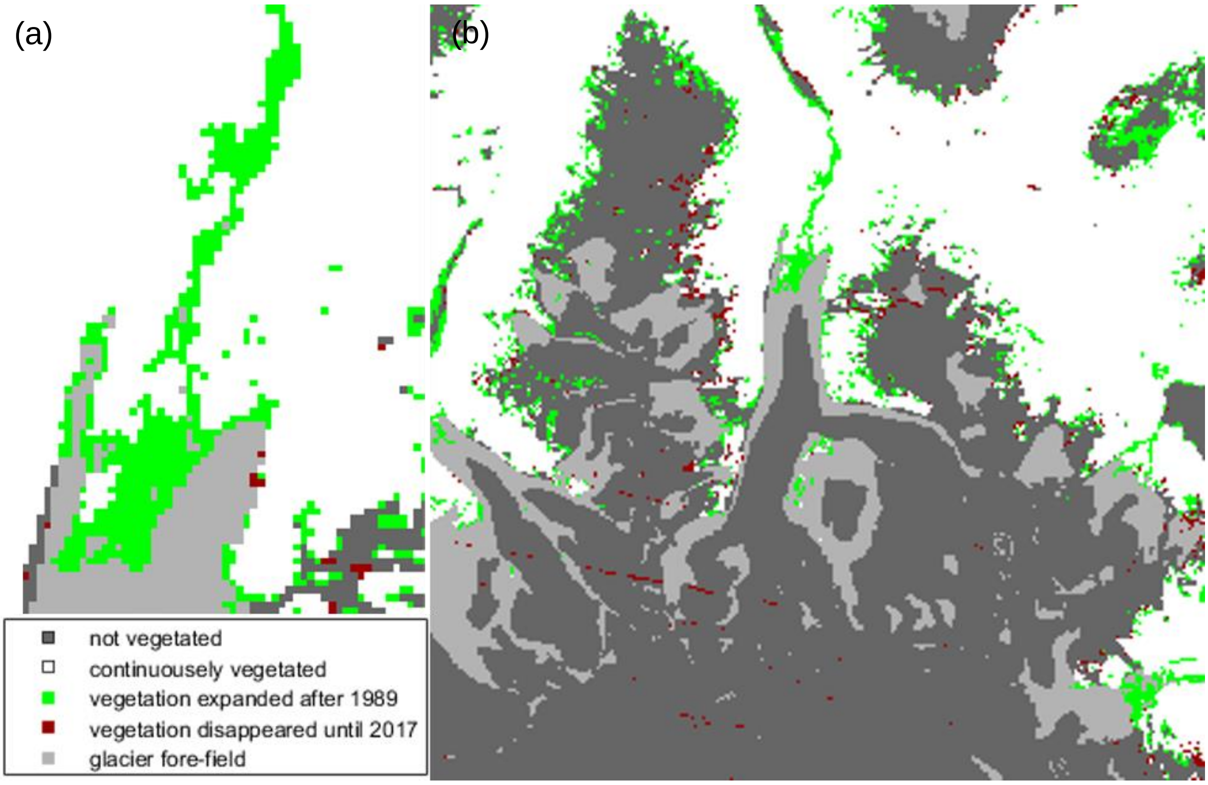

Figure 20: Changes in the extent of primary vegetation. (a) shows a closer view on the tip of the Morteratsch glacier fore-field while the pro-glacial in a wider view is displayed in (b). Areas into which primary vegetation expanded between 1989 and 2017 are marked in green, areas from which primary vegetation disappeared between 1989 and 2017 are marked in dark red. White areas were classified as primary vegetation in both 1989 and 2017 and dark grey areas were classified neither in 1989 nor in 2017.

Complementing the previous map, Figure 21 shows the changes in the extent of developed vegetation in the Morteratsch region between 1989 and 2017. Dark grey areas make up most of the image and the white areas which were classified as developed vegetation in both 1989 and 2017 are located mostly at the valley bottom. The red areas are sparse and are found mostly in some patches in the transition zone between dark grey and white. The green areas now mark locations where NDVI values above 0.6 were found only in 2017 but not in 1989. They are in this region by far more abundant than the red areas. The close-up on the tip of the Morteratsch pro-glacial area reveals hardly any developed vegetation in 1989 (white or red areas) and a considerable amount of green areas of new, developed vegetation.

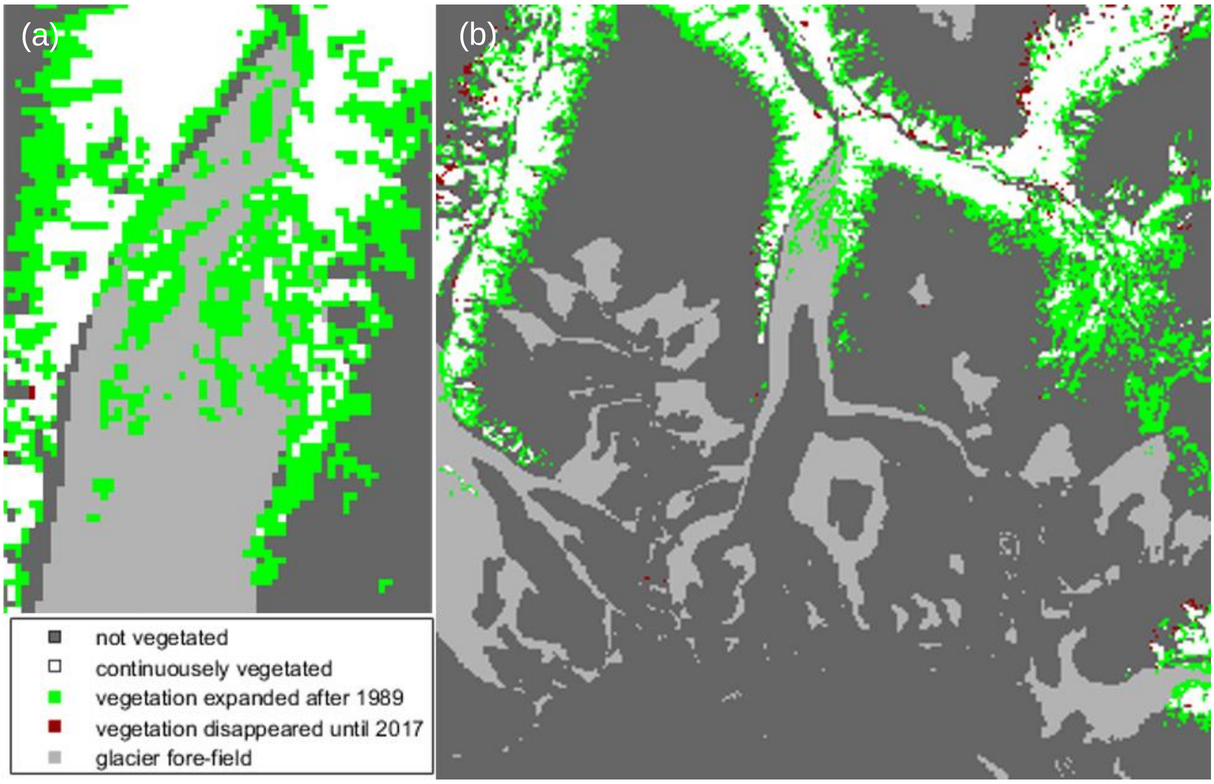

Figure 21: Changes in the extent of developed vegetation. (a) shows a closer view on the tip or the Morteratsch glacier fore-field while the pro-glacial in a wider view is displayed on the (b). Areas into which developed vegetation expanded between 1989 and 2017 are marked in green, areas from which developed vegetation disappeared between 1989 and 2017 are marked in dark red. White areas were classified as developed vegetation in both 1989 and 2017 and dark grey areas were classified neither in 1989 nor in 2017.

Figure 22 shows expansion of vegetation in the Morteratsch area between 1990 and 2015 relative to the size of the pro-glacial area. The expansion of primary vegetation is shown in (a) and indicates an expansion of about 10% for the larger glaciers such as the Morteratsch glacier in the centre of the image or the Tschierva glacier on the left border of the image. The smaller pro-glacial areas show a variable response. Some indicate high expansion, some hardly any. The expansion of developed vegetation shown in (b) also indicates no negative values. The smaller pro-glacial areas higher up the valleys show no expansion and the glacier fore-fields lower in the valley show a moderate expansion. Notably, the Morteratsch glacier fore-field shows a higher expansion of developed vegetation than primary vegetation.

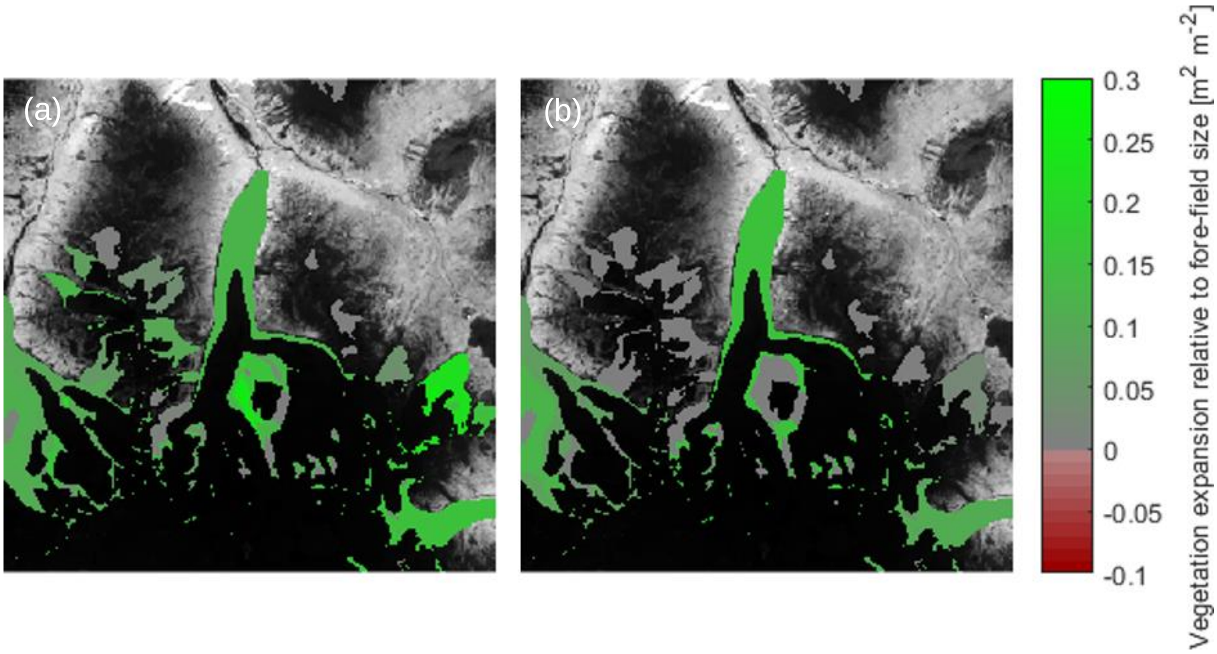

Figure 22: Expansion of primary (a) and developed (b) vegetation relative to glacier fore-field size in the area of the Morteratsch pro-glacial area. The values are calculated for each pro-glacial area as the area of vegetation expansion between 1990 and 2015 divided by the size of the pro-glacial area.

The plots in Figure 23 bring the results from Figure 22 to the scale of the Swiss Alps The single pro-glacial areas displayed in Figure 22 are represented in Figure 23 as individual dots together with every other glacial fore-field part of the Swiss Alps. As derived from the DEM shown in Figure 13, the glacier fore-fields range from 980 to 4540 m a.s.l. with a mean elevation of 2700 m a.s.l. The areas of the glacier fore-fields, as calculated from the shapefiles, range from 900 m^2 (one pixel) to 17.3 km^2 (ca. 20’000 pixels) with a mean of 0.3 km^2 (290 pixels). The location of the glacier fore-fields in the Swiss Alps is displayed in Appendix 4. The plots show the vegetation expansion relative to the size of the glacier fore-field in the context of the mean altitude in m a.s.l. (a) and size of the pro-glacial area in m^2 (b). The expansion of primary vegetation shows a high spread for altitudes up to about 3000 m a.s.l. It also shows some individual, negative values. Expansion in areas higher than 3500 m a.s.l. area close to zero. When compared to the size of the pro-glacial area, a higher spread is found for smaller pro-glacial areas. The expansion of developed vegetation generally shows lower values than the expansion of primary vegetation. When compared to the mean altitude of the pro-glacial area, the spread is similarly high but there are hardly any expansion values above zero over an altitude of 3000 m a.s.l. The expansion of developed vegetation also shows a higher spread for smaller pro-glacial areas and the biggest glacier fore-fields have positive expansions in both primary and developed vegetation.

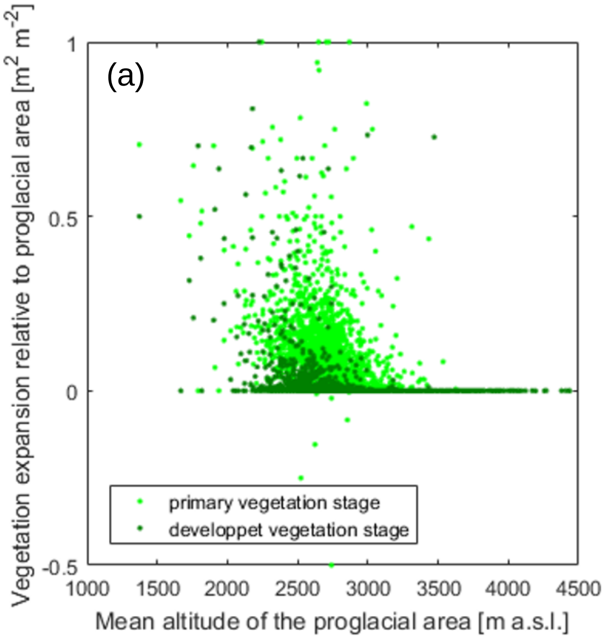

Figure 23: Scatterplots showing the expansion of primary (light green) and developed (dark green) vegetation relative to glacier fore-field size for all Swiss glacier fore-fields plotted against the mean altitude (a) and size (b) of the respective pro-glacial area.

4.2 Temporal evolution of vegetation expansion

Figure 24 shows the cumulative frequency of the time passing between terrain exposure and vegetation growth considering the growth of primary vegetation (a) and of developed vegetation (b). Generally, growth of primary vegetation occurs earlier than the growth of developed vegetation. Many pro-glacial areas show considerable growth of primary vegetation in about the first 30 years after exposure while the bulk of the growth of developed vegetation occurred about 100 and 150 years after exposure. There are predominantly smaller pro-glacial areas in which growth of primary vegetation also takes distinctly longer than 30 to 50 years. Only a few small glaciers show an early growth of developed vegetation.

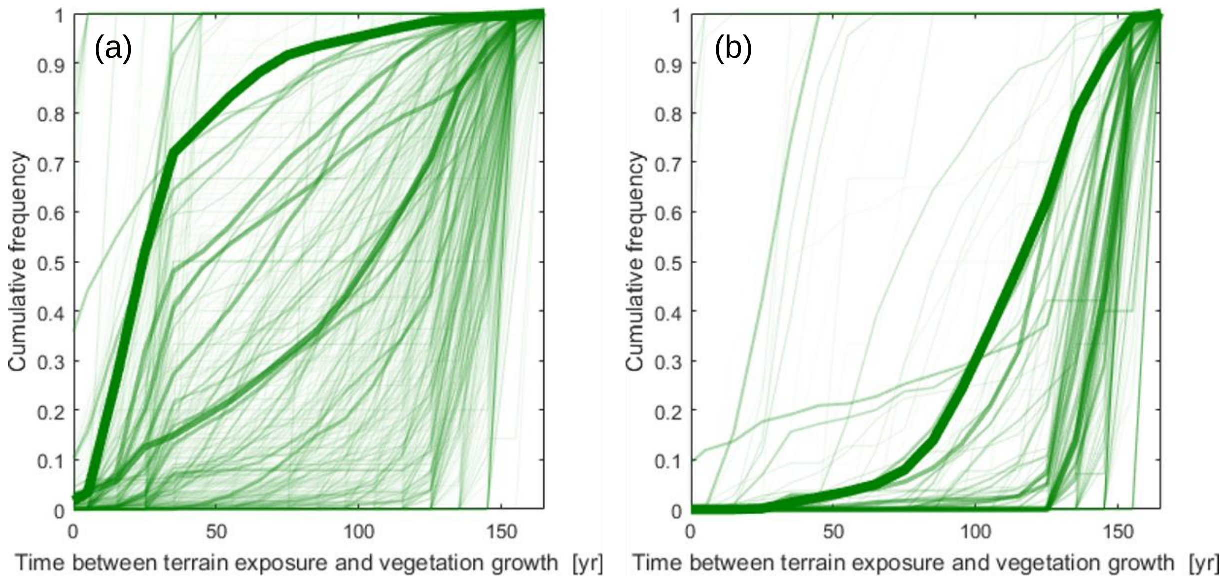

Figure 24: Cumulative frequency of the time in years between terrain exposure and vegetation growth for all Swiss glacier fore-fields shown for primary (a) and developed (b) vegetation succession. The cumulative frequency was calculated in groups of 10 years. The size of the glacier fore-field is reflected in the thickness and colour intensity of the line. The frequency is normalized to the vegetated area of the respective glacier fore-field.

As a first step towards calculating the difference in rates of vegetation expansion of the period 1850 to 1990 and 1850 to 2010, the number of pixels classified as vegetation at the end of the period is displayed in Figure 25. The spatial extent of the glacier fore-field, in which the pixels classified as vegetation were counted was set to the outlines of 1973 for the first period and to the outlines of 2010 for the second period. The choice of the border of the pro-glacial area is also represented in the figure. The total number of pixels classified as vegetation increased both for primary (a to b) and developed (c to d) vegetation. Number are by trend higher for primary vegetation and for larger glacier fore-fields.

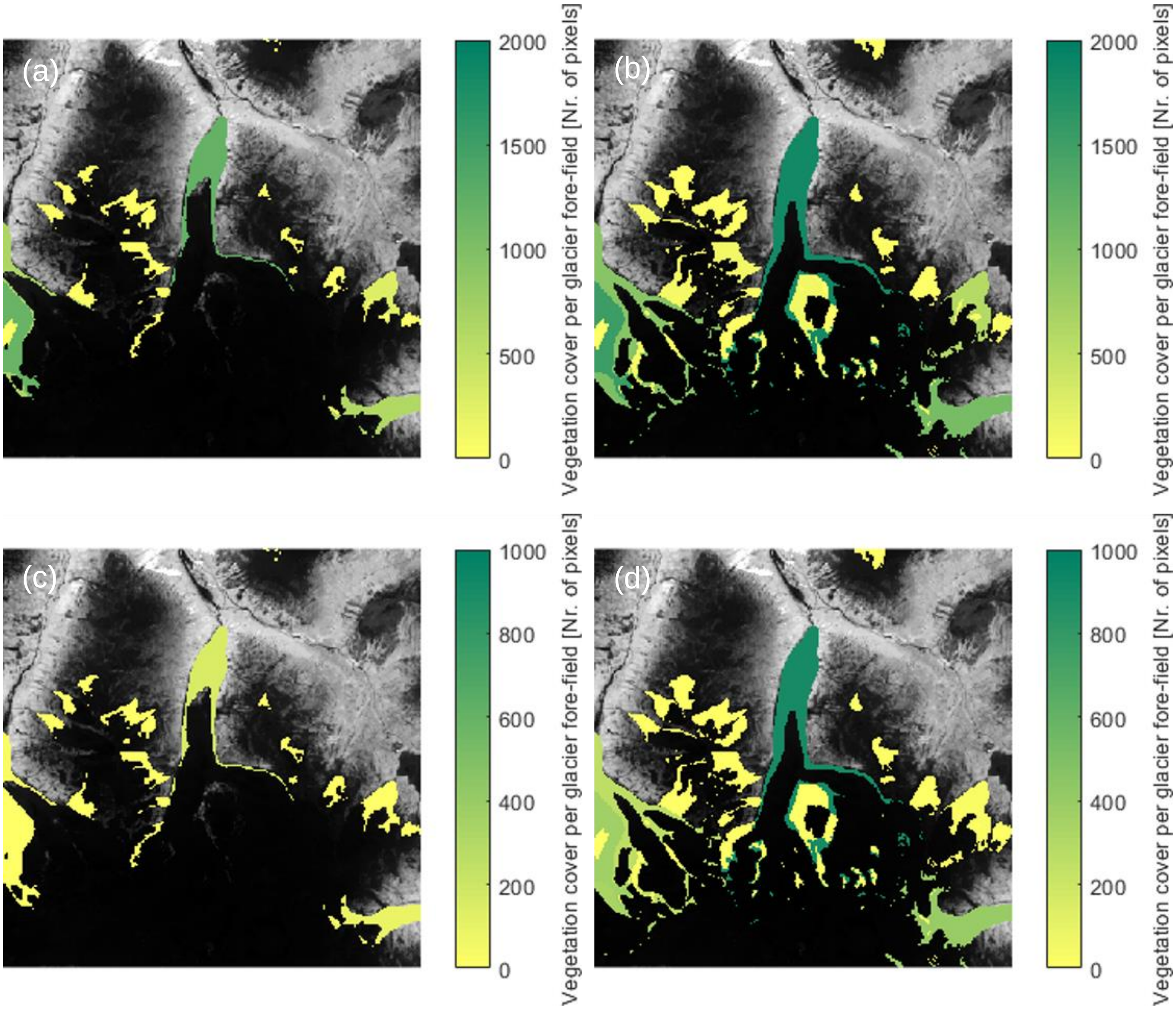

Figure 25: Number of pixels classified as vegetation for each glacier fore-field given for primary vegetation and the glacier fore-field until 1990 (a), for primary vegetation until 2015 (b), for developed vegetation until 1990 (c) and for developed vegetation until 2010 (d). For values until the year 1990, the extent of the glacier fore-field in 1973 was used and for values until the year 2015, the extent of the glacier fore-field in 2010 was used.

The figure displaying the number of pixels classified as vegetation normalized by the area of the glacier fore-field is shown in Appendix 5. The normalisation was performed with the same extents of the pro-glacial areas as in the counting of pixels in Figure 25. Thus, Appendix 5 shows the fraction of the area becoming ice-free during 140 years (a, c) or 165 years (b, d) with was classified as vegetation at the end of the concerned period. Normalisation by the duration of the time span resulted in the annual rate of relative vegetation cover, as displayed in Figure 26. For the Morteratsch glacier fore-field, the rate is highest for the growth of primary vegetation between 1850 and1990 and lowest for the growth of developed vegetation between 1850 and 2010.

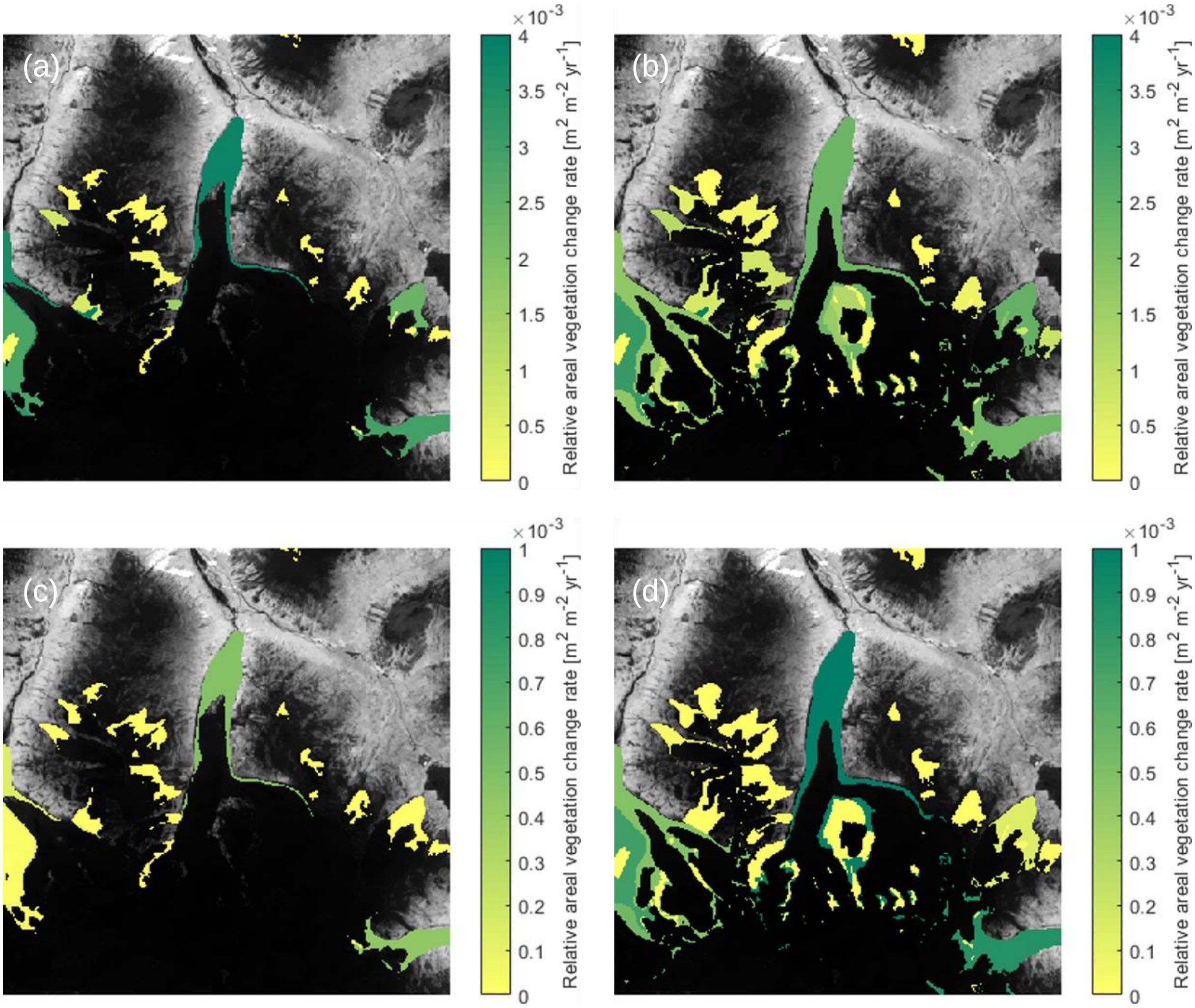

Figure 26 Relative areal vegetation change rate for each glacier fore-field given for primary vegetation and the glacier fore-field until 1990 (a), for primary vegetation until 2015 (b), for developed vegetation until 1990 (c) and for developed vegetation until 2010 (d). For values until the year 1990, the extent of the glacier fore-field in 1973 was used and for values until the year 2015, the extent of the glacier fore-field in 2010 was used.

In Figure 27, the differences in rates of vegetation expansion of the period 1850 to 1990 (Figure 26, b minus a) and the period 1850 to 2015 (Figure 26, d minus c) is shown with respect to primary vegetation (a) and developed vegetation (b). The larger pro-glacial areas reaching further into the valleys such as the Morteratsch or Tschierva pro-glacial areas show a decrease in the expansion rate of primary vegetation from the first to the second period while the smaller glaciers further up show variable changes. Contrary, the larger pro-glacial areas show an increase in the expansion rate of developed vegetation while the smaller pro-glacial areas often show no change in the expansion rate. However, it is not clear for some small areas whether they count as part of the larger pro-glacial areas or on their own.

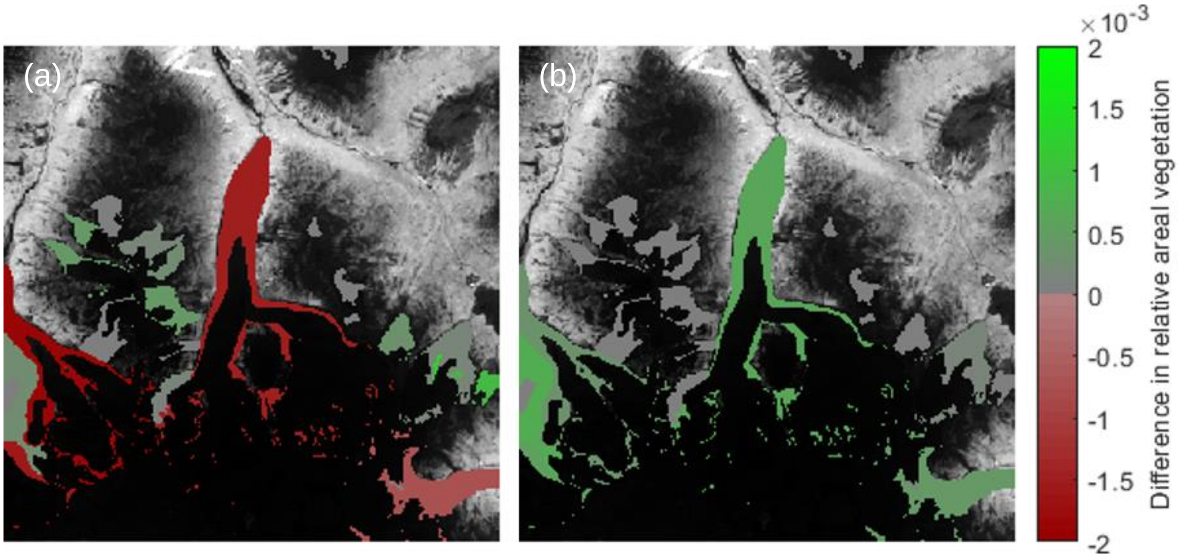

Figure 27: Difference in the annual rate of vegetation expansion relative to glacier fore-field area between the periods 1850 – 1990 and 1850 – 2015 shown for primary (a) and developed (b) vegetation succession in the Morteratsch region. Positive values shown in green colours indicate a faster vegetation expansion for the period 1850 – 2015 while negative values shown in red colours indicate a slower vegetation expansion for the period 1850 – 2015.

After Figure 27 illustrated the difference in the relative annual vegetation expansion rates in the area of the Morteratsch glacier, Figure 28 shows the differences on the scale of the Swiss Alps. The rate differences are plotted against the mean altitude of the respective pro-glacial area (a) and against the size of the pro-glacial area (b). The expansion rates of primary vegetation changed variably for pro-glacial areas with mean altitudes below about 3000 m a.s.l. and showed only a slight increase in higher areas. Increases in the expansion rate of primary vegetation increased rather for smaller glacier fore-fields while more of the larger pro-glacial areas experienced decreases.

The expansion rates of developed vegetation generally changed less with the bulk of the pro-glacial areas showing no change or a slight increase. The spread of the changes is increased for pro-glacial areas below 2500 to 3000 m a.s.l. In contrast, there are hardly any changes in the rate difference in higher elevations. There are some distinct increases in the expansion rates of developed vegetation for smaller glacier fore-fields and the larger pro-glacial areas show most of the decreasing rates but also some increases. One-sided t-tests confirmed that the differences in expansion rates of both primary and developed vegetation are both significantly above 0 at the 5% significance level. For the difference in relative vegetation expansion rate for primary vegetation, a mean value of 3.1E-04 $m^2m^{-2}y^{-1}$ was confirmed above zero with a p-value of 1.22E-66 while for developed vegetation, a mean value of 7.33E-05 $m^2m^{-2}y^{-1}$ and a p-value of 2.55E-19 was calculated.

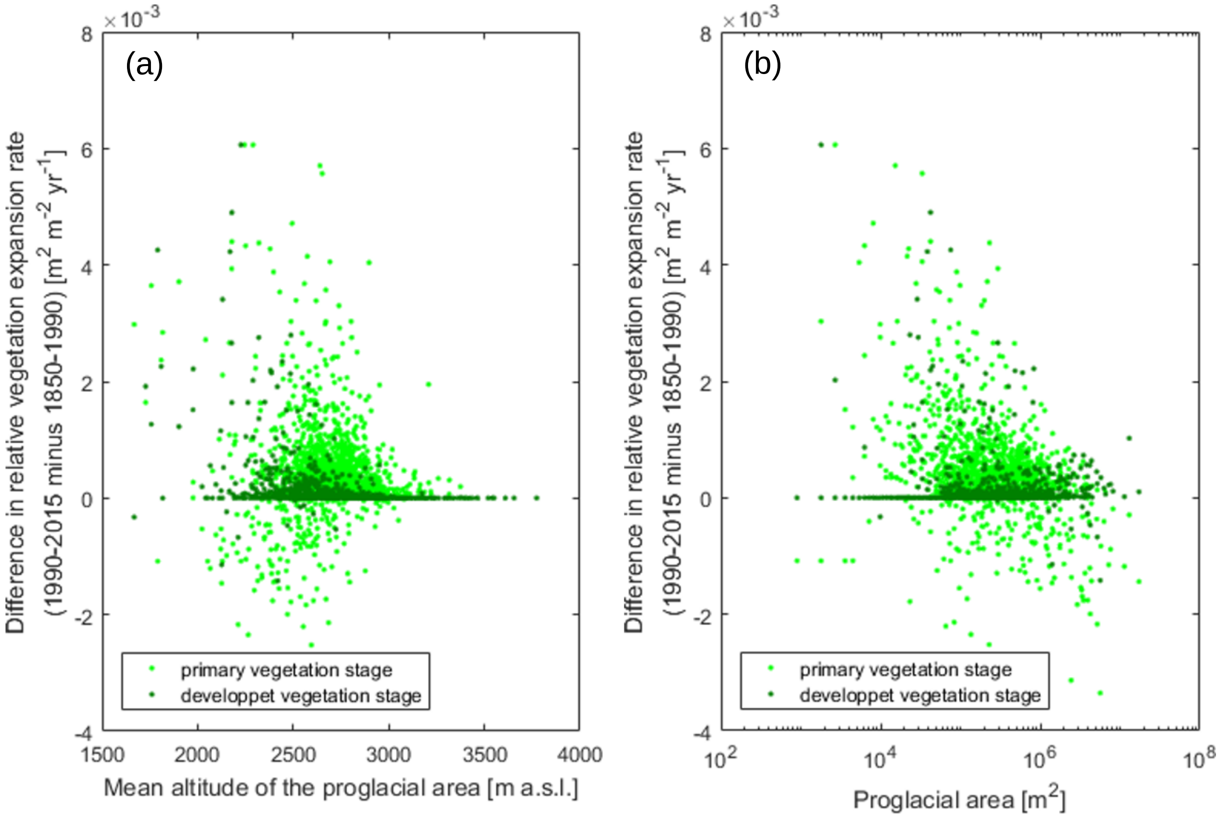

Figure 28: The difference in the annual rate of vegetation expansion relative to glacier fore-field area between the periods 1850 – 1990 and 1850 – 2015 for primary (light green) and developed (dark green) vegetation succession of all Swiss glacier fore-fields is plotted against the mean altitude (a) and size (b) of the respective pro-glacial area.

5. Discussion

5.1 Detection of vegetation

Vegetation in the Morteratsch glacier fore-field was mostly tracked well by NDVI where it was said or expected to occur according to Figure 4 and Figure 7 (a, b). As visible in Figure 7 and Figure 8 (c), NDVI reached the highest values where the surface is covered by vegetation with no other natural surface cover or clouds reaching similarly high values, thus agreeing with literature (Beck et al., 2006; Myneni et al., 1997). There are scenes during a year with missing information about vegetation cover as clouds obscured the glacier fore-field, only parts of the pro-glacial area were covered by the satellite image or NDVI was decreased through reduced biological activity, e.g. during cold spring or autumn days (different possibilities illustrated in Figure 9). The exclusion of these effects worked well with the chosen approach to extract the 95-percentile NDVI value per year for each pixel on the glacier fore-fields. As a comparison, Brown et al. (2006) used a similar approach with success. However, as mentioned in the Methods chapter, artefacts of high NDVI-values can occur. As shown in Appendix 6, the NDVI composite in 1984 in the area of the Morteratsch glacier still contained such structures, even though the top 5% of the NDVI values were excluded. A lower percentage value could have been used to exclude further artefacts, but at the cost of information about high NDVI values in other places.

Comparing the NDVI at the tip of the Morteratsch glacier fore-field (Figure 10, b) with a vegetation map of this region (Figure 4) shows that higher NDVI values between 0.5 and 0.7 are found in the area of Green Alder scrub (see Figure 29, a). Lower NDVI values of 0.2 to 0.4 are found in the earlier successional stages of Epilobietum fleischeri (see Figure 29, b) cover. Non-vegetated areas show a NDVI value below 0.2. With the size of a single pixel being 900 m², NDVI values are interpreted rather as indications of vegetation density than as indications of individual plant activity or health. The different vegetation classes from Figure 4 contain some differences in vegetation density, as shrub species as the Green Alder scrub often consist of more layers with a higher horizontal extent than herb species such as Epilobietum fleischeri. These examples of different vegetation cover illustrate a possible land cover in areas where the respective NDVI values occur and support the validity of the approach chosen in this study. Smaller scaled comparison of NDVI values and vegetation classes were made difficult by the coarse resolution of the satellite images as mixed pixels and neighbouring effects prevent a clear assignment of a range of NDVI values to vegetation classes without larger, continuous areas. The areas not directly comparable to a vegetation map in Figure 10 agree with the expectation of generally lower NDVI values in the upper part of the mountain valleys, a visible difference between the area outside of the Morteratsch glacier fore-field and the pro-glacial area itself with its distinctly lower terrain age. Primary vegetation (Figure 11, a) reached higher up the mountain valleys, spread extensively in the lower glacier fore-fields and was found even in some of the higher pro-glacial areas while developed vegetation (Figure 11, b) were neither expected nor found (with isolated exceptions) in the higher parts of the valleys above the timberline.

Figure 29: Picture of and Green Alder Scrub (a, source: e-ecodb.bas.bg) and Epilobietum fleischeri (b, source: flora.nhm-wien.ac.at).

The extents of primary and developed vegetation base on a threshold classification and thus rely on the quality of the thresholds. A NDVI-threshold of 0.6 for developed vegetation has been used as an attempt to combine different settings of mixed-pixels, which are considered as vegetation developed further than just the primary succession. Pixels with a NDVI of about 0.6 may represent a mostly vegetated area, but vegetation activity is only intermediate. Another possibility would be a fraction of the area covered by highly active vegetated compensated by bare area combining to a NDVI of about 0.6. In between, various combinations of different vegetation activities and share of vegetation cover are possible. However, the use of the annual 95-percentile NDVI value is supposed to catch most vegetation close to their maximum activity. With the assumption that the degree of vegetation cover has the higher impact on the measured NDVI values than the maximum NDVI of the different plant species, a threshold of 0.6 is in the first place attributed rather to the density of vegetation cover than to a vegetation type. However, vegetation types of the later succession such as larger scrubs or trees require a certain density of vegetation to build up a suitable environment (soil thickness, substrate stability). Thus, the area classified as developed vegetation at least has a higher change of containing plants of the later succession.

Although a threshold of 0.1 on NDVI tracks some vegetation that are ignored with higher thresholds such as 0.2 or even 0.3, it also includes by mistake vegetation-free areas and classifies it as vegetation. A threshold of 0.3 classifies even more area that is actually vegetated as no vegetation when compared to a lower threshold, but most of the pixels classified contain vegetation. A comparison of the classification with thresholds 0.1, 0.2 and 0.3 in the Morteratsch area for the 95-percentile NDVI-values of the year 2017 is displayed in Appendix 7. Thus, the threshold of 0.2 for primary vegetation was chosen as a trade-off between errors of the first and second kind, whether the presence of any vegetation is tracked correctly.

5.2 Extent of vegetation expansion

The extent of expanding vegetation distinctly outweighs the decreases in vegetation cover. The changes in NDVI between 1989 and 2017 as shown in Figure 19 are highest in the lower ends of the larger pro-glacial areas that reach furthest into the valley. The decreases in the higher areas are only of low amplitude. As most of these areas in pale red are not classified as vegetation in Figure 20, these changes are less attributed to changes in vegetation but rather to subtle differences between low NDVI values. However, there are processes reducing vegetation cover that can also occur on the glacier fore-field that are mostly morphodynamical and decrease in likeliness with increasing vegetation cover as the substrate gets stabilized.

The expansion of primary vegetation in the Morteratsch glacier fore-field as shown in Figure 20 mostly imply an extension of the vegetation cover towards the glacier and the glacial stream into areas, where the considered vegetation type has not yet been present. This migration towards higher elevations is not only found in the glacier fore-fields, but in most of the areas in Figure 20 and Figure 21, supporting studies finding upward migration of vegetation in the European Alps based on historic data (Pauli et al., 2014) and models (Gottfried et al., 1999). However, within this upward shift, developed migration (Figure 21) shows the additional behaviour of expanding around isolated areas that are already covered by developed vegetation. This is indicated by green areas surrounding white spots as in the tip of the Morteratsch pro-glacial area or on in Figure 21 (b). A similar behaviour was reported by Gehrig-Fasel et al. (2007) who found most increases of forest cover within previous forest borders for the Swiss Alps between 1650 and 2450 m a.s.l. This ingrowth, as it is referred to by literature, is supposedly less prominent in pro-glacial areas, as there are less shrubs and trees to densify the cover.

The expansion of primary vegetation in the larger glaciers shows signs of saturation. As indicated in Figure 20, the tip of the Morteratsch glacier fore-field is to a large part already covered with vegetation and the area for primary vegetation to expand got limited over time. Figure 22 shows for the Morteratsch glacier fore-field a lower expansion for primary than for developed vegetation, suggesting that this saturation effect is less pronounced for developed vegetation (Figure 21, a): some dark grey area was left in 2017 for developed vegetation to expand further). This might also be an explanation of the decrease in the expansion of primary vegetation for larger pro-glacial areas (Figure 23, b). However, the effect is diluted, as larger pro-glacial areas require larger absolute vegetation expansion to result in high relative expansion values when compared to smaller glacier fore-fields, where a few pixels can have a high impact on the relative changes. For the plot of relative vegetated area versus glacier size as displayed in Figure 23 (b), the interval for glacier size is 900 m^2 (one pixel). As the calculation of the relative area is also based on the number of pixels, there is only a discrete number of values for relative area for small glacier fore-fields. In the logarithmic plot, this results in gaps between lines of data for smaller pro-glacial areas that are caused by the discretisation and thus with no meaning as regards to content. Within the plot, the largest glaciers, which accordingly require stronger vegetation expansion to show high relative values, all show at least some expansion of developed vegetation as within their large extent they are expected to reach areas of lower elevation, which are more favourable to the growth of shrubs and trees.

The vegetation expansion is generally limited to pro-glacial areas below 3500 m a.s.l. for primary vegetation (Figure 23, a) and below 3000 m a.s.l. for developed vegetation (Figure 23, b), as higher elevations get less favourable for vegetation growth with decreasing temperature. Vegetation expansion in elevations lower than this threshold shows a high variability. This can be explained due to variable conditions affecting vegetation expansion such as elevation and aspect (Körner, 2003), soil stabilization (Temme, 2019), acidity and carbonate content of the substrate (Arnesen et al., 2007), proximity to the glacier (Matthews, 1992) and proximity to other vegetated areas (Erschbamer et al., 2008; Nagl and Erschbamer, 2010).

5.3 Vegetation expansion in the context of time

The growth of primary vegetation generally starts early, but the bulk of it was detected on a large spread of terrain ages. On many pro-glacial areas, primary vegetation was detected within the first few decades. Literature reports vegetation growth during the first few years (Matthews, 1992; Nagl and Erschbamer, 2010). On the Morteratsch glacier fore-field, Epilobietum fleischerli, Oxyria digyna and Achillea mocidua were found after 5-8 yeas as pioneer species (Maisch et al., 1993). After 10 to 15 years, several herb species such as Avenella flexuosa or Poa alpine were reported with some fern species growing between rock boulders and moss cushions covering fine sands (Maisch et al., 1993). This is not necessarily confirmed by the results in Figure 24. Even though, there was primary vegetation detected within the first years after glacier retreat, sometimes even before, there are still errors in the estimation of terrain age displayed in Figure 14 which may cause these results. Partially, the errors arise from the geometry of the glacier fore-field. In an elongated tip for the glacier fore-field, the density of points from the LIA outline is higher than in a broad section. In the case of the larger glaciers and primary vegetation, this is supposed to have only a minor effect on the duration between glacier retreat and vegetation detection as the tip was already mostly vegetated. For developed vegetation, this might have caused a higher difference between the terrain age and the time of vegetation detection which was not fully compensated by other effects as developed vegetation was predominately detected in the tongues of the glacier fore-fields. As a further aspect of uncertainty, a few small, isolated pioneer plants which can be detected in the field do not necessarily result in a NDVI value above 0.2 on a pixel with a size of 30 m. Thus, the first vegetation might in fact have grown earlier than the results in Figure 24 (a), as a NDVI of 0.2 was not yet reached. The large spread of terrain age at which growth was detected in the case of primary vegetation with some smaller glaciers only showing over 120 years after glacier retreat, suggests a dependence on site specific factors, comparable to the different environmental conditions explaining the high variability in vegetation expansion in the previous section. However, colouring the lines of the plot with respect to the mean elevation of the glacier fore-field revealed no clear trend (see Appendix 8).

Shrub species are reported by literature to start growing after 40-80 years without glacier cover (Lüdi, 1958; Maisch et al., 1993; Nagl and Erschbamer, 2010; Raffl et al., 2006), which agrees with the results shown in Figure 24 (b). But most of the growth of developed vegetation occurs over 100 years after glacier retreat. This agrees with Lüdi (1958) and Maisch et al. (1993), who reported that a loose forest takes over 100 years without glacier cover to grow and coincides with soil respiration rates reaching after the same time. While the information about the timing of vegetation growth shown in Figure 24 is mostly but a confirmation of previous knowledge, they add satellite derived time series of a vegetation index as a new approach and the entirety of the glacier fore-fields in the Swiss Alps as a new scale to complement previous results.

The changes in the annual rates of primary and developed vegetation expansion between the periods 1850 to 1990 and 1850 to 2015 fit to the various effects of climate change and glacier fore-field dynamics on vegetation expansion. Even though there were decreases in the rate of primary vegetation expansion found for the Morteratsch (Figure 27, a) and several other glaciers Figure 28, light green), most of the glaciers showed increases expansion rates, also in the case of developed vegetation (Figure 28, dark green). The increase in the expansion of developed vegetation is also consistent with larger shrub expansion rates found in alpine environments (Cannone et al., 2007). Additionally, there was an increasing abundance of thermophilic species reported above the timberlines in European mountains between 2001 and 2008 (Gottfried et al., 2012), which also hints towards vegetation adapting towards warmer conditions in higher elevations. Supported by the results of the student-t test, which confirm that the changes of annual vegetation expansion rates of both primary and developed vegetation are significantly positive, these results suggest, that the pro-glacial areas had rather improved as habitats for vegetation between 1990 and 2015, but not in every case.

Climate change has affected the Swiss Aps with surface temperatures rising by about 0.5°C (Harris, 2003) and air temperature increasing by up to 2°C within the 20th century (Beniston, 2008, 2012). With the warming causing stronger glacier retreats since the late 20th century (Fischer et al., 2014, 2015; Zemp et al., 2008), there is generally also additional meltwater entering the pro-glacial area during the summer months. The environmental changes have both negative and positive effects on plant growth in the alpine environments (Pauli et al., 2014). As an example, the reduction of snow cover due to increased air temperature benefits alpine grassland species but limits the growth of frost-sensitive species that rely on the isolating effect of the snow cover (Pauli et al., 1999, 2014).

Unfortunately, there is a discrepancy forced by the available data between the years limiting the examined periods and the extent of the considered pro-glacial areas with the period 1850 – 1990 evaluated for the glacier fore-field 1850 – 1973 and the period 1850 – 2015 for the fore-field limited by the extents of the glaciers in 1850 and 2010. As the shifts are both towards too small glacier extents for the considered period and with the result on the scale of the Swiss Alps being quite robust, the difference in the vegetation growth rates are still considered to agree with a positive effect of climate change on vegetation growth in pro-glacial areas on the large scale.

6. Conclusion

In this thesis, a time series of optical satellite data was combined with shapefiles of the glacier extents and a digital terrain model to analyse the dynamics of vegetation in the glacier fore-fields of the Swiss Alps. The use of a threshold classification on yearly composites of satellite-derived NDVI values provided a flexible tool to track the extent of vegetation in different stages while facing several trade-offs. The percentile to derive the yearly NDVI composite was chosen as a balance between determining the signal of maximum vegetation activity and reducing the impact of artefacts within the data. The threshold value used for the detection of primary vegetation was a trade-off between avoiding the classification of non-vegetated areas as vegetation and tracking even small signals of vegetation. The threshold value for developed vegetation cannot concludingly be assigned to a successional state as intermediate NDVI values can be interpreted ambiguously. Nevertheless, comparison with a vegetation map of a test region and consideration of the classification-based extents of vegetated areas supported the feasibility of the approach. However, even with the use of the 95-percentile to derive the annual NDVI composite, the first years of the dataset were mostly being obscured by artefacts.

Most pro-glacial areas were found to show considerable growth of primary vegetation after about 30 years without glacier cover. As the threshold for the detection of primary vegetation was set to a NDVI of 0.2, some earlier occurrences might have been missed, hinting towards an even lower duration. Developed vegetation was detected mostly between 100 and 150 years after exposure. However, the estimation of the terrain age was too high by trend in the tongues of the glacier fore-fields where developed vegetation was predominately detected. This resulted in a longer duration between glacier retreat and detection of developed vegetation, thus the results of 100 to 150 years might be on the higher end.

The changes between the time from 1850 to the start of the satellite measurements and last 30 years in the glacier fore-fields of the Swiss Alps was analysed in the context of changes along gradients of elevation and size of the pro-glacial area. By trend, large glacier fore-fields showed a decrease in the expansion rate of primary vegetation. This could have been caused by situations where most of the area easy to colonize had already been covered by plans and the space for primary vegetation to extend further was simply limited. On the contrary, the larger pro-glacial areas showed an increase in the expansion of developed vegetation. Smaller glacier fore-fields below 3000 m a.s.l. showed an increase in the expansion rate of primary vegetation while above, changes were rather small. Overall, the pro-glacial areas were found to have improved conditions for the growth of both primary and developed vegetation. The difference in the annual rate of relative vegetation change was 3.1E-04 $m^2m^{-2}y^{-1}$ for primary vegetation and was significantly above zero with a p-value of 1.22E-66 while the difference for developed vegetation was 7.33E-05 $m^2m^{-2}y^{-1}$ with a p-value of 2.55E-19. With the assumption that vegetation grows in successively higher elevations, even a constant rate of vegetation expansion hints towards effects of climate change, as the effect of colder conditions in higher elevations is being counteracted.

This thesis was a first attempt to systematically assess vegetation dynamics within the glacier fore-fields of the Swiss Alps. For further analysis, site-specific information such as slope, aspect, incoming radiation or climatology should be concerned as parameters of explanatory value for vegetation expansion which can be obtained in the scale of the Swiss Alps. A comparison with Sentinel 2 data from recent years potentially allows assessments on a finer local scale. With remote sensing applications continuing to spread, this thesis affirms the practicability of assessments of vegetation succession based on time series of satellite data.

Acknowledgements

I would like to thank the supervisors Dr. Frank Paul and Dr. Rogier De Jong for the counsel and feedback given to support me in this master's thesis.

References

Arnesen, G., Beck, P.S.A., & Engelskjøn, T. (2007). Soil Acidity, Content of Carbonates, and Available Phosphorus Are the Soil Factors Best Correlated with Alpine Vegetation: Evidence from Troms, North Norway. *Arctic, Antarctic, and Alpine Research*, *39*, 189–199.

Beck, P.S.A., Atzberger, C., Høgda, K.A., Johansen, B., & Skidmore, A.K. (2006). Improved monitoring of vegetation dynamics at very high latitudes. A new method using MODIS NDVI. *Remote Sensing of Environment*, *100*, 321–334.

Beniston, M. (2008). Sustainability of the landscape of a UNESCO World Heritage Site in the Lake Geneva region (Switzerland) in a greenhouse climate. *International Journal of Climatology*, *28*, 1519–1524.

Beniston, M. (2012). Impacts of climatic change on water and associated economic activities in the Swiss Alps. *Journal of Hydrology*, *412-413*, 291–296.

Berdwell, T., Dugmore, A.J., & SugdenE, D.E. (2008). The Little Ice Age glacier maximum in Iceland and the North Atlantic Oscillation. Evidence from Lambatungnajökull, southeast Iceland. *Boreas*, *35*, 61–80.

Brown, M.E., Pinzon, J.E., Didan, K., Morisette, J.T., & Tucker, C.J. (2006). Evaluation of the consistency of long-term NDVI time series derived from AVHRR,SPOT-vegetation, SeaWiFS, MODIS, and Landsat ETM+ sensors. *IEEE Transactions on Geoscience and Remote Sensing*, *44*, 1787–1793.

Burga, C.A. (1999). Vegetationsdynamik in Gletschervorfeldern der Schweizer Zentralalpen am Beispiel von Morteratsch (Pontresina, Graubünden, Schweiz). *Berich. Reinh. Tüxen-Gesell*, *11*, 267–277.

Burga, C.A., Krüsi, B., Egli, M., Wernli, M., Elsener, S., Ziefle, M., Fischer, T., & Mavris, C. (2010). Plant succession and soil development on the foreland of the Morteratsch glacier

(Pontresina, Switzerland). Straight forward or chaotic? *Flora - Morphology, Distribution, Functional Ecology of Plants*, *205*, 561–576.
Cannone, N., Diolaiuti, G., Guglielmin, M., & Smiraglia, C. (2008). ACCELERATING CLIMATE CHANGE IMPACTS ON ALPINE GLACIER FOREFIELD ECOSYSTEMS IN THE EUROPEAN ALPS. *Ecological Applications*, *18*, 637–648.
Cannone, N., Sgorbati, S., & Guglielmin, M. (2007). Unexpected impacts of climate change on alpine vegetation. *Frontiers in Ecology and the Environment*, *5*, 360–364.
Carrivick, J., Heckmann, T., Fischer, M., & Davies, B. (2019). An inventory of proglacial systems in Austria, Switzerland and across Patagonia. Landform and sediment dynamics in recently deglaciated alpine landscapes. In (pp. 43–57).
Cía, J.C., Andrés, A.J., Sánchez, M.S., Novau, J.C., & Moreno, J.L. (2005). Responses to climatic changes since the Little Ice Age on Maladeta Glacier (Central Pyrenees). *Geomorphology*, *68*, 167–182.
Duveiller, G., Hooker, J., & Cescatti, A. (2018). The mark of vegetation change on Earth's surface energy balance. *Nature Communications*, *9*, 679.
Egli, M., Wernli, M., Burga, C., Kneisel, C., Mavris, C., Valboa, G., Mirabella, A., Plötze, M., & Haeberli, W. (2011). Fast but spatially scattered smectite-formation in the proglacial area Morteratsch: An evaluation using GIS. *Geoderma*, *164*, 11–21.
Eichel, J. (2019). Vegetation Succession and Biogeomorphic Interactions in Glacier Forelands. In T. Heckmann, & D. Morche (Eds.), *Geomorphology of Proglacial Systems: Landform and Sediment Dynamics in Recently Deglaciated Alpine Landscapes* (pp. 327–349). Cham: Springer International Publishing.
Ellenberg, H., & Leuschner, C. (2010). *Vegetation Mitteleuropas mit den Alpen: in ökologischer, dynamischer und historischer Sicht:* Utb.
Erschbamer, B., Niederfriniger Schlag, R., & Winkler, E. (2008). Colonization processes on a central Alpine glacier foreland. *Journal of Vegetation Science*, *19*, 855–862.
Fischer, A., Seiser, B., Stocker Waldhuber, M., Mitterer, C., & Abermann, J. (2015). Tracing glacier changes in Austria from the Little Ice Age to the present using a lidar-based high-resolution glacier inventory in Austria. *The Cryosphere*, *9*, 753–766.
Fischer, M., Huss, M., Barboux, C., & Hoelzle, M. (2014). The New Swiss Glacier Inventory SGI2010. Relevance of Using High-Resolution Source Data in Areas Dominated by Very Small Glaciers. *Arctic, Antarctic, and Alpine Research*, *46*. https://doi.org/10.1657/1938-4246-46.4.933.
Fischer, T. (1999). *Waldgrenzökoton und Wiederbewaldungsdynamik im Gebiet des Morteratschgletschers:* Verlag nicht ermittelbar.
Flood, N. (2014). Continuity of Reflectance Data between Landsat-7 ETM+ and Landsat-8 OLI, for Both Top-of-Atmosphere and Surface Reflectance. A Study in the Australian Landscape. *Remote Sensing*, *6*. http://www.mdpi.com/2072-4292/6/9/7952.
Freudiger, D., Mennekes, D., Seibert, J., & Weiler, M. (2018). Historical glacier outlines from digitized topographic maps of the Swiss Alps for the years ca. 1900 and ca. 1935.
Galvão, L.S., Breunig, F.M., Teles, T.S., Gaida, W., & Balbinot, R. (2016). Investigation of terrain illumination effects on vegetation indices and VI-derived phenological metrics in subtropical deciduous forests. *GIScience & Remote Sensing*, *53*, 360–381.
Gehrig-Fasel, J., Guisan, A., & Zimmermann, N.E. (2007). Tree line shifts in the Swiss Alps. Climate change or land abandonment? *Journal of Vegetation Science*, *18*, 571–582.
Gottfried, M., Pauli, H., Reiter, K., & Grabherr, G. (1999). A fine-scaled predictive model for changes in species distribution patterns of high mountain plants induced by climate warming. *Diversity and Distributions*, *5*, 241–251.
Grove, J.M. (2013). *Little ice ages: Ancient and modern, second edition*.
Haeberli, W. (1995). Climate change impacts on glaciers and permafrost. *Potential Ecological Impacts of Climate Change in the Alps and Fennoscandian Mountains: Geneva University Press, Geneva*, 97–103.

Hagg, W., Mayer, C., Mayr, E., & Heilig, A. (2012). Climate and glacier fluctuations in the Bavarian Alps in the past 120 years. *Erdkunde*, 121–142.

Hall, M.H.P., & Fagre, D.B. (2003). Modeled Climate-Induced Glacier Change in Glacier National Park, 1850–2100. *BioScience*, *53*, 131–140.

Hannesdóttir, H., Björnsson, H., Pálsson, F., Aðalgeirsdóttir, G., & Guðmundsson, S. Variations of southeast Vatnajökull ice cap (Iceland) 1650–1900 and reconstruction of the glacier surface geometry at the Little Ice Age maximum. *Geografiska Annaler: Series A, Physical Geography*, *97*, 237–264.

Harris, C. (2003). Warming permafrost in European mountains. *Global and Planetary Change*, *39*, 215–225.

Harrison, B.A., & Jupp, D.L.B. (1989). *Introduction to Remotely Sensed Data:* CSIRO Australia, Division of Water Resources.

Jochimsen, M. (1962). Das Gletschervorfeld-keine Wüste. *Jb. Österr. Alpenver*, *87*, 135–142.

Körner, C. (2003). *Alpine plant life: functional plant ecology of high mountain ecosystems; with 47 tables:* Springer Science & Business Media.

Luckman, B.H. (2000). The Little Ice Age in the Canadian Rockies. *Geomorphology*, *32*, 357–384.

Lüdi, W. (1958). Beobachtungen über die Besiedlung von Gletschervorfeldern in den Schweizeralpen. *Flora oder Allgemeine Botanische Zeitung*, *146*, 386–407.

Magnusson, J.O. (2012). Hydrological response of a glacier forefield to meteorological forcing on diurnal, seasonal and decadal time scales.

Maisch, M. (2000). *Die Gletscher der Schweizer Alpen. Gletscherhochstand 1850, aktuelle Vergletscherung, Gletscherschwund-Szenarien.* Zürich: vdf.

Maisch, M., Burga, C.A., & Fitze, P. (1993). *Lebendiges Gletschervorfeld. Von schwindenden Eisströmen, schuttreichen Moränenwällen und wagemutigen Pionierpflanzen im Vorfeld des Morteratschgletschers : Führer und Begleitbuch zum Gletscherlehrpfad Morteratsch:* Gemeinde Pontresina.

Marcante, S., Winkler, E., & Erschbamer, B. (2009). Population dynamics along a primary succession gradient: do alpine species fit into demographic succession theory? *Annals of Botany*, *103*. https://dx.doi.org/10.1093/aob/mcp047.

Marti, R., Gascoin, S., Houet, T., Ribière, O., Laffly, D., Condom, T., Monnier, S., Schmutz, M., Camerlynck, C., Tihay, J.P., Soubeyroux, J.M., & René, P. (2015). Evolution of Ossoue Glacier (French Pyrenees) since the end of the Little Ice Age. *The Cryosphere*, *9*, 1773–1795.

Matsushita, B., Yang, W., Chen, J., Onda, Y., & Qiu, G. (2007). Sensitivity of the Enhanced Vegetation Index (EVI) and Normalized Difference Vegetation Index (NDVI) to Topographic Effects. A Case Study in High-density Cypress Forest. *Sensors (Basel, Switzerland)*, *7*, 2636–2651.

Matthews, J.A. (1992). *The ecology of recently-deglaciated terrain: a geoecological approach to glacier forelands:* Cambridge University Press.

Matthews, J.A., & Vater, A.E. (2015). Pioneer zone geo-ecological change: Observations from a chronosequence on the Storbreen glacier foreland, Jotunheimen, southern Norway. *CATENA*, *135*, 219–230.

Montague, T., & Kjelgren, R. (2004). Energy balance of six common landscape surfaces and the influence of surface properties on gas exchange of four containerized tree species. *Scientia Horticulturae*, *100*, 229–249.

Myneni, R.B., & Asrar, G. (1994). Atmospheric effects and spectral vegetation indices. *Remote Sensing of Environment*, *47*, 390–402.

Myneni, R.B., Keeling, C.D., Tucker, C.J., Asrar, G., & Nemani, R.R. (1997). Increased plant growth in the northern high latitudes from 1981 to 1991. *Nature*, *386*. https://doi.org/10.1038/386698a0.

Nagl, F., & Erschbamer, B. (2010). Kapitel 6. Pflanzliche Sukzessionen im Gletschervorfeld. Vegetation und Besiedlungsstrategien. *Glaziale und periglaziale Lebensräume im Raum Obergurgl. Innsbruck University press, Innsbruck*, 121–142.
Nordberg, M.-L., & Evertson, J. (2005). Vegetation index differencing and linear regression for change detection in a Swedish mountain range using Landsat TM® and ETM+® imagery. *Land Degradation & Development*, *16*, 139–149.
Paul, F., & Bolch, T. (2019). Glacier Changes Since the Little Ice Age. In T. Heckmann, & D. Morche (Eds.), *Geomorphology of Proglacial Systems: Landform and Sediment Dynamics in Recently Deglaciated Alpine Landscapes* (pp. 23–42). Cham: Springer International Publishing.
Paul, F., Kääb, A., Maisch, M., Kellenberger, T., & Haeberli, W. (2002). The new remote-sensing-derived Swiss glacier inventory. I. Methods. *Annals of Glaciology*, *34*, 355–361.
Pauli, H., Gottfried, M., & Grabherr, G. (1999). Vascular plant distribution patterns at the low temperature limits of plant life - the alpine-nival ecotone of Mount Schrankogel (Tyrol, Austria). *Phytocoenologia*, *29*, 297–325.
Pauli, H., Gottfried, M., & Grabherr, G. (2014). Effects of climate change on the alpine and nival vegetation of the Alps. *Journal of Mountain Ecology*, *7*. http://www.mountainecology.org/index.php/me/article/view/134/117.
Rabatel, A., Francou, B., Jomelli, V., Naveau, P., & Grancher, D. (2008). A chronology of the Little Ice Age in the tropical Andes of Bolivia (16°S) and its implications for climate reconstruction. *Quaternary Research*, *70*, 198–212.
Raffl, C., Mallaun, M., Mayer, R., & Erschbamer, B. (2006). Vegetation Succession Pattern and Diversity Changes in a Glacier Valley, Central Alps, Austria. *Arctic, Antarctic, and Alpine Research*, *38*, 421–428.
Regmi, P., Grosse, G., Jones, M., Jones, B., & Anthony, K. (2012). Characterizing Post-Drainage Succession in Thermokarst Lake Basins on the Seward Peninsula, Alaska with TerraSAR-X Backscatter and Landsat-based NDVI Data. *Remote Sensing*, *4*, 3741–3765.
Robbins, J.A., & Matthews, J.A. (2018). Regional Variation in Successional Trajectories and Rates of Vegetation Change on Glacier Forelands in South-Central Norway. *Arctic, Antarctic, and Alpine Research*, *42*, 351–361.
Roy, D.P., Kovalskyy, V., Zhang, H.K., Vermote, E.F., Yan, L., Kumar, S.S., & Egorov, A. (2016). Characterization of Landsat-7 to Landsat-8 reflective wavelength and normalized difference vegetation index continuity. *Remote Sensing of Environment*, *185*, 57–70.
Roy, D.P., Wulder, M.A., Loveland, T.R., C.E., W., Allen, R.G., Anderson, M.C., Helder, D., Irons, J.R., Johnson, D.M., Kennedy, R., Scambos, T.A., Schaaf, C.B., Schott, J.R., Sheng, Y., Vermote, E.F., Belward, A.S., Bindschadler, R., Cohen, W.B., Gao, F., Hipple, J.D., Hostert, P., Huntington, J., Justice, C.O., Kilic, A., Kovalskyy, V., Lee, Z.P., Lymburner, L., Masek, J.G., McCorkel, J., Shuai, Y., Trezza, R., Vogelmann, J., Wynne, R.H., & Zhu, Z. (2014). Landsat-8. Science and product vision for terrestrial global change research. *Remote Sensing of Environment*, *145*, 154–172.
Schumann, K., Gewolf, S., & Tackenberg, O. (2016). Factors affecting primary succession of glacier foreland vegetation in the European Alps. *Alpine Botany*, *126*, 105–117.
Song, C., Woodcock, C.E., Seto, K.C., Lenney, M.P., & Macomber, S.A. (2001). Classification and Change Detection Using Landsat TM Data. When and How to Correct Atmospheric Effects? *Remote Sensing of Environment*, *75*, 230–244.
Stow, D.A., Hope, A., McGuire, D., Verbyla, D., Gamon, J., Huemmrich, F., Houston, S., Racine, C., Sturm, M., Tape, K., Hinzman, L., Yoshikawa, K., Tweedie, C., Noyle, B., Silapaswan, C., Douglas, D., Griffith, B., Jia, G., Epstein, H., Walker, D., Daeschner, S., Petersen, A., Zhou, L., & Myneni, R. (2004). Remote sensing of vegetation and land-cover change in Arctic Tundra Ecosystems. *Remote Sensing of Environment*, *89*, 281–308.

Swisstopo (2018). swissALTI3D Ausgabebericht 2018, Bundesamt für Landestopografie swisstopo.

Teillet, P.M., Barker, J.L., Markham, B.L., Irish, R.R., Fedosejevs, G., & Storey, J.C. (2001). Radiometric cross-calibration of the Landsat-7 ETM+ and Landsat-5 TM sensors based on tandem data sets. *Remote Sensing of Environment*, *78*. http://www.sciencedirect.com/science/article/pii/S0034425701002486.

Teillet, P.M., & Staenz, K. (2014). Atmospheric Effects Due to Topography on Modis Vegetation Index Data Simulated from Aviris Imagery over Mountainous Terrain. *Canadian Journal of Remote Sensing*, *18*, 283–291.

Temme, A.J.A.M. (2019). The Uncalm Development of Proglacial Soils in the European Alps Since 1850. In T. Heckmann, & D. Morche (Eds.), *Geomorphology of Proglacial Systems: Landform and Sediment Dynamics in Recently Deglaciated Alpine Landscapes* (pp. 315–326). Cham: Springer International Publishing.

Tresch, E. (2007). Hydrochemistry of the Damma glacier forefield. temporal and spatial variability.

Vaughan, D.G., Cosimo, J.C., Allison, I., Carrasco, J., Kaser, G., Kwok, R., Mote, P., Murray, T., Paul, F., Ren, J., Rignot, E., Solomina, O., Steffen, K., & Zhang, T. (2013). : Observations: Cryosphe. In Stocker, T.F., D. Qin, G.-K. Plattner, M. Tignor, S.K. Allen, J. Boschung, A. Nauels, Y. Xia, V. Bex and P.M. Midgley (eds.) (Ed.), *n: Climate Change 2013: The Physical Sci-ence Basis. Contribution of Working Group I to the Fifth Assessment Report of the Intergovernmental Panel on Climate Change.* Cambridge, United Kingdom and New York, NY, USA: Cambridge University Press.

Vogelmann, J.E., Helder, D., Morfitt, R., Choate, M.J., Merchant, J.W., & Bulley, H. (2001). Effects of Landsat 5 Thematic Mapper and Landsat 7 Enhanced Thematic Mapper Plus radiometric and geometric calibrations and corrections on landscape characterization. *Remote Sensing of Environment*, *78*, 55–70.

Walker, D.A., Auerbach, N.A., & Shippert, M.M. (1995). NDVI, biomass, and landscape evolution of glaciated terrain in northern Alaska. *Polar Record*, *31*, 169.

Wanner, H., Beer, J., Bütikofer, J., Crowley, T.J., Cubasch, U., Flückiger, J., Goosse, H., Grosjean, M., Joos, F., Kaplan, J.O., Küttel, M., Müller, S.A., Prentice, I.C., Solomina, O., Stocker, T.F., Tarasov, P., Wagner, M., & Widmann, M. (2008). Mid- to Late Holocene climate change. An overview. *Quaternary Science Reviews*, *27*, 1791–1828.

Weidmann, Y., Gandor, F., & Artuso, R. (2019). Temporale Metadaten swissALTI3D. Die Zeit als zusätzliche Dimension des Höhenmodells. In *Geoinformatik Schweiz* (pp. 306–310).

Zekollari, H., Fürst, J.J., & Huybrechts, P. (2014). Modelling the evolution of Vadret da Morteratsch, Switzerland, since the Little Ice Age and into the future. *J. Glaciol*, *60*, 1155–1168.

Zemp, M., Paul, F., Hoelzle, M., & Haeberli, W. (2008). Glacier fluctuations in the European Alps, 1850–2000. An overview and spatio-temporal analysis of available data: University of California Press.

Zhao, B., Yan, Y., Guo, H., He, M., Gu, Y., & Li, B. (2009). Monitoring rapid vegetation succession in estuarine wetland using time series MODIS-based indicators. An application in the Yangtze River Delta area. *Ecological Indicators*, *9*, 346–356.

Appendix

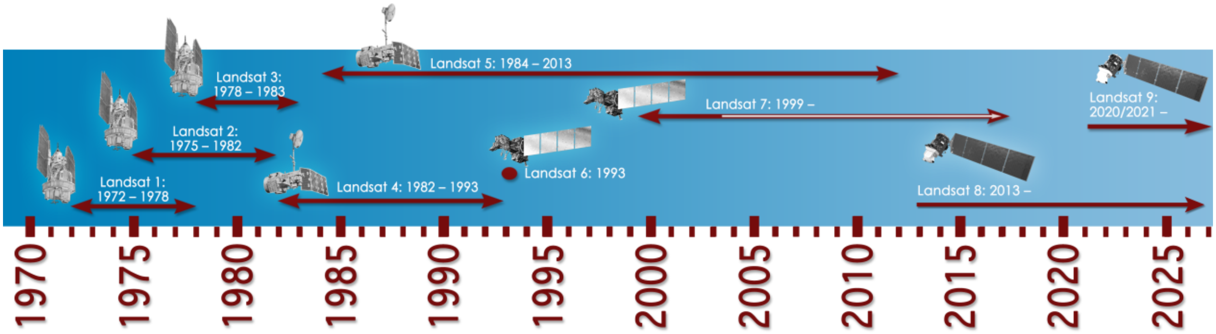

Appendix 1: Timeline of the Landsat series of satellites (source: https://landsat.gsfc.nasa.gov/a-landsat-timeline/).

MSS Bands			**TM Bands**		
Band Number	**µm**	**Resolution**	**Band Number**	**µm**	**Resolution**
			1	0.45-0.52	30 m
1	0.5-0.6	68 m X 83 m	2	0.52-0.60	30 m
2	0.6-0.7	68 m X 83 m	3	0.63-0.69	30 m
3	0.7-0.8	68 m X 83 m	4	0.76-0.90	30 m
4	0.8-1.1	68 m X 83 m	5	1.55-1.75	30 m
			6	10.41-12.5	120 m
			7	2.08-2.35	30 m

Appendix 2: Table of the spectral bands of the Multispectral Scanner System (MSS) and Thematic Mapper (TM) of Landsat 5 (source: https://landsat.gsfc.nasa.gov/landsat-5/).

Landsat-7 ETM+ Bands (μm)			Landsat-8 OLI and *TIRS* Bands (μm)		
			30 m Coastal/Aerosol	0.435 - 0.451	Band 1
Band 1	30 m Blue	0.441 - 0.514	30 m Blue	0.452 - 0.512	Band 2
Band 2	30 m Green	0.519 - 0.601	30 m Green	0.533 - 0.590	Band 3
Band 3	30 m Red	0.631 - 0.692	30 m Red	0.636 - 0.673	Band 4
Band 4	30 m NIR	0.772 - 0.898	30 m NIR	0.851 - 0.879	Band 5
Band 5	30 m SWIR-1	1.547 - 1.749	30 m SWIR-1	1.566 - 1.651	Band 6
Band 6	60 m TIR	10.31 - 12.36	*100 m TIR-1*	*10.60 – 11.19*	Band 10
			100 m TIR-2	*11.50 – 12.51*	Band 11
Band 7	30 m SWIR-2	2.064 - 2.345	30 m SWIR-2	2.107 - 2.294	Band 7
Band 8	15 m Pan	0.515 - 0.896	15 m Pan	0.503 - 0.676	Band 8
			30 m Cirrus	1.363 - 1.384	Band 9

Appendix 3: Table of the spectral bands of the Enhanced Thematic Mapper Plus (ETM+) of Landsat 7 and Operational Land Imager (OLI) and Thermal instrument (TIRS) of Landsat 8 (source: https://landsat.gsfc.nasa.gov/landsat-data-continuity-mission/).

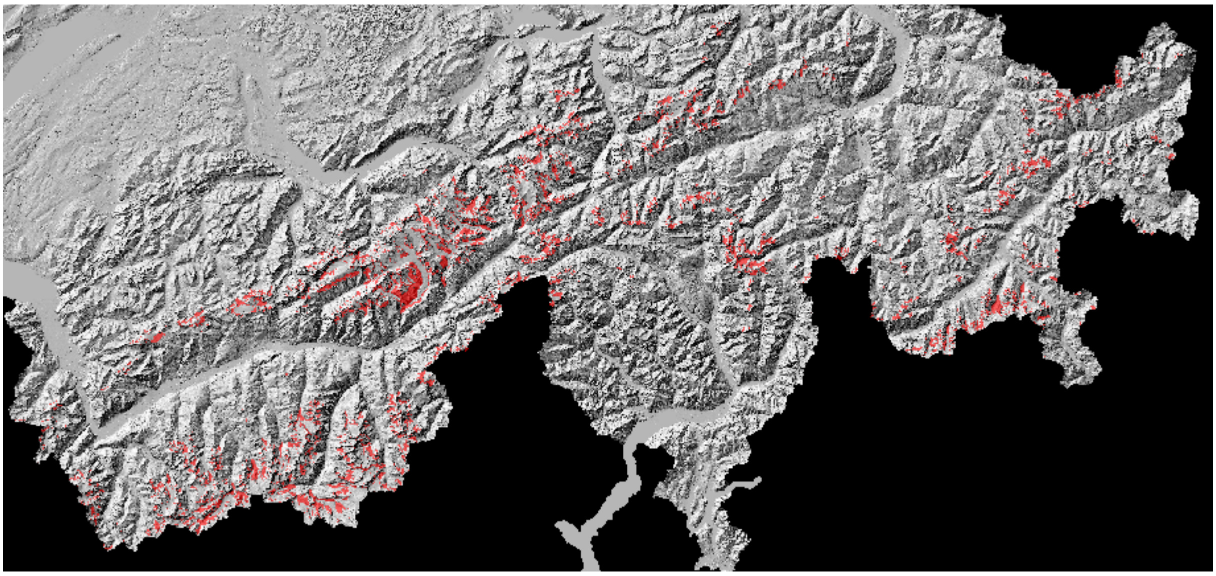

Appendix 4: Location of the glacier fore-fields (in red) in the Swiss Alps displayed on the hillshade data from SwissALTI3d (Swisstopo, 2018).

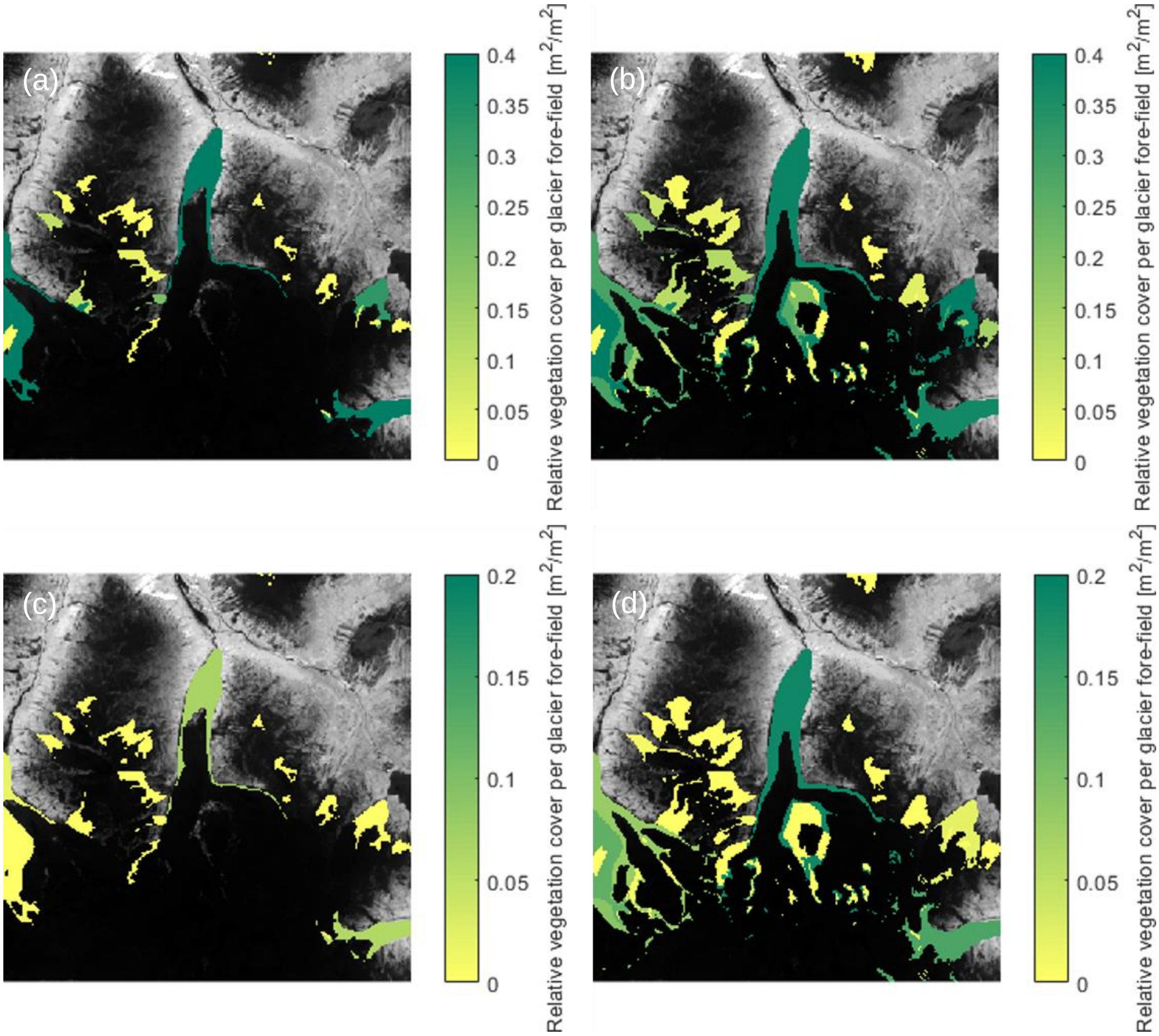

Appendix 5: Relative vegetation cover for each glacier fore-field given for primary vegetation and the glacier fore-field until 1990 (a), for primary vegetation until 2015 (b), for developed vegetation until 1990 (c) and for developed vegetation until 2010 (d). For values until the year 1990, the extent of the glacier fore-field in 1973 was used and for values until the year 2015, the extent of the glacier fore-field in 2010 was used.

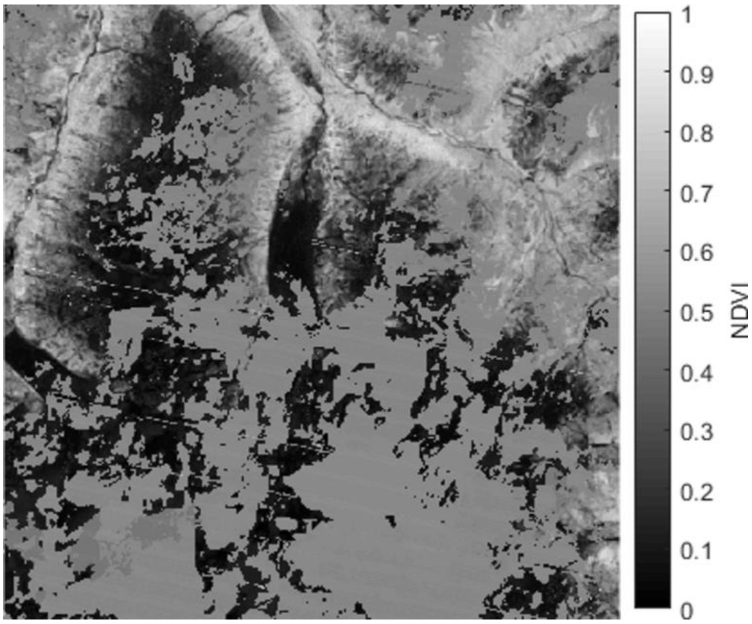

Appendix 6: The NDVI composed of the 95-percentlie NDVI values in the region of the Morteratsch glacier for the year 1984.

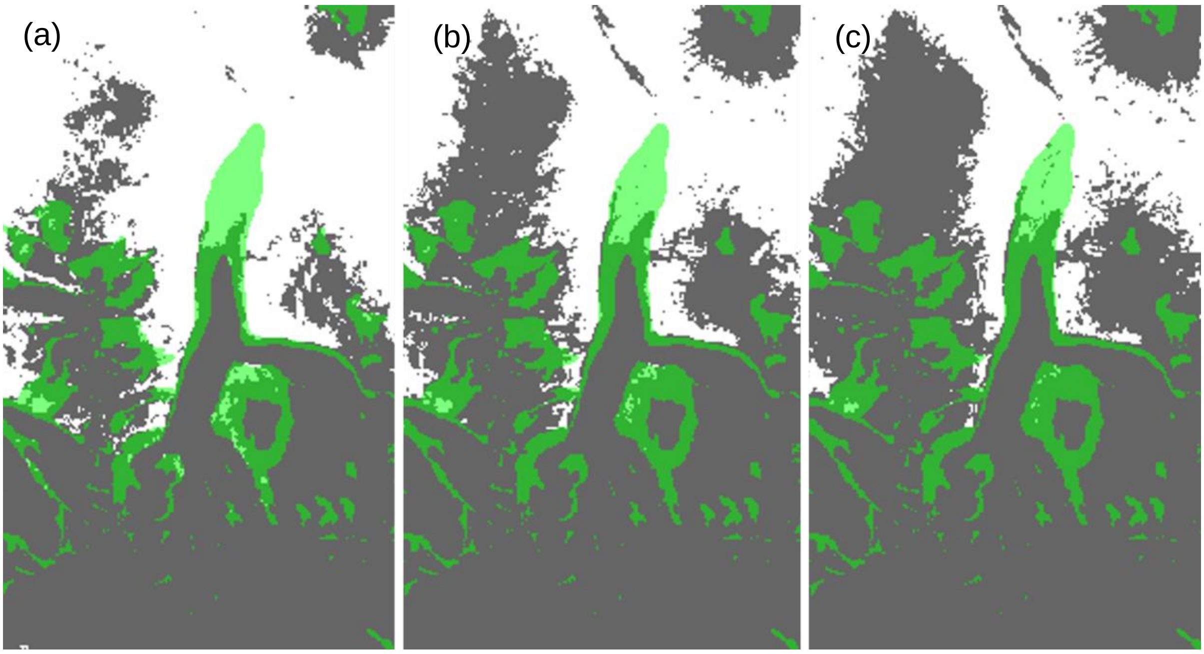

Appendix 7: Comparison of the threshold classification on NDVI > 0.1 (a), NDVI > 0.2 (b) and NDVI > 0.3 (c) for the year 2017 in the area of the Morteratsch glacier. White areas were classified as vegetated and dark grey areas as not vegetated. The extent of the glacier fore-fields is overlain in green.

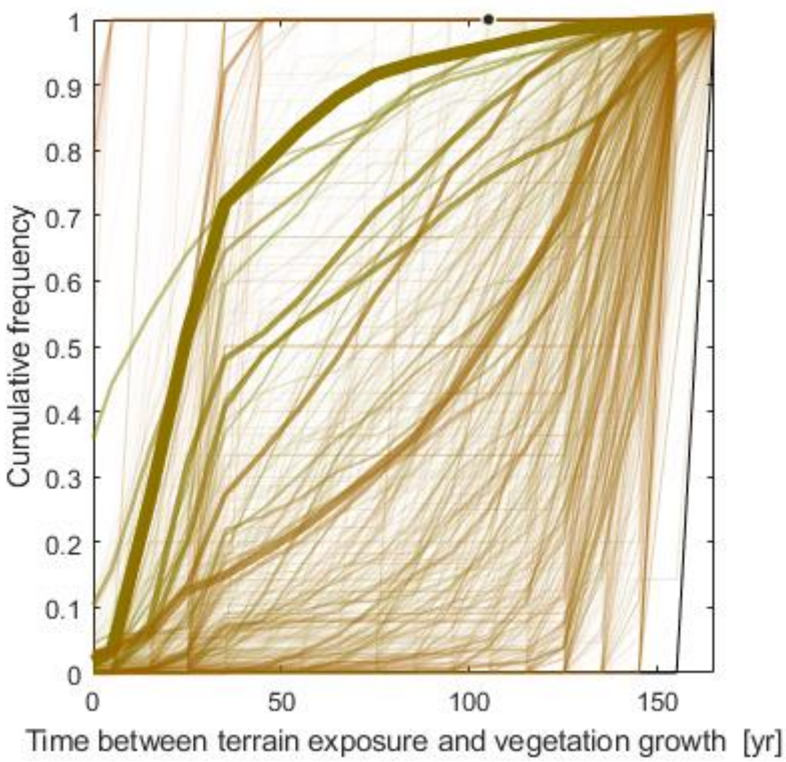

Appendix 8: Cumulative frequency of the time in years between terrain exposure and vegetation growth for all Swiss glacier fore-fields shown for primary vegetation succession. The cumulative frequency was calculated in groups of 10 years. The colour of the lines represents the mean elevation of the pro-glacial area ranging from green (the lower glacier fore-fields) to red (the higher fore-fields). The size of the glacier fore-field is reflected in the thickness and colour intensity of the line. The frequency is normalized to the vegetated area of the respective glacier fore-field.

Personal declaration: I hereby declare that the submitted thesis is the result of my own, independent work. All external sources are explicitly acknowledged in the thesis.

S. Röthlin

Zürich, 29.06.2019